Manuscript Details

Manuscript number	ATMOSRES_2017_121
Title	Intense air-sea exchanges and heavy orographic precipitation over Italy: the role of Adriatic Sea surface temperature uncertainty
Article type	Research Paper

Abstract

Strong and persistent low-level winds blowing over the Adriatic basin are often associated with intense precipitation events over Italy. Typically, in case of moist southeasterly wind (Sirocco), rainfall affects northeastern Italy and the Alpine chain, while with cold northeasterly currents (Bora) precipitations are localized along the eastern slopes of the Apennines and central Italy coastal areas. These events are favoured by intense air-sea interactions and it is reasonable to hypothesize that the Adriatic Sea surface temperature (SST) can affect the amount and location of precipitation. High-resolution simulations of different Bora and Sirocco events leading to severe precipitation are performed using a convection-permitting model (MOLOCH). Sensitivity experiments varying the SST initialization field are performed with the aim of evaluating the impact of SST uncertainty on precipitation forecasts, which is a relevant topic for operational weather predictions, especially at local scales. Moreover, diagnostic tools to compute water vapour fluxes across the Italian coast and atmospheric water budget over the Adriatic Sea have been developed and applied in order to characterize the air mass that feeds the precipitating systems. Finally, the investigation of the processes through which the SST influences location and intensity of heavy precipitation allows to gain a better understanding on mechanisms conducive to severe weather in the Mediterranean area and in the Adriatic basin in particular. Results show that the effect of the Adriatic SST (uncertainty) on precipitation is complex and can vary considerably among different events. For both Bora and Sirocco events, SST does not influence markedly the atmospheric water budget or the degree of moistening of air that flows over the Adriatic Sea. SST mainly affects the stability of the atmospheric boundary layer, thus influencing the flow dynamics and the orographic flow regime, and in turn, the precipitation pattern.

Keywords	Heavy precipitation; SST; air-sea interaction; orography; water budget
Manuscript category	Mesoscale meteorology and numerical modelling

Corresponding Author	Paolo Stocchi
Corresponding Author's Institution	ISAC-CNR
Order of Authors	Paolo Stocchi, Silvio Davolio
Suggested reviewers	Cindy Lebeaupin Brossier, kristian Horvath

Intense air-sea exchanges and heavy orographic precipitation over Italy: the role of Adriatic Sea surface temperature uncertainty

Paolo Stocchi, Silvio Davolio

National Research Council of Italy, Institute of Atmospheric Sciences and Climate (CNR – ISAC), Bologna, Italy

Corresponding author: Paolo Stocchi, P.Stocchi@isac.cnr.it

Abstract

Strong and persistent low-level winds blowing over the Adriatic basin are often associated with intense precipitation events over Italy. Typically, in case of moist southeasterly wind (Sirocco), rainfall affects northeastern Italy and the Alpine chain, while with cold northeasterly currents (Bora) precipitations are localized along the eastern slopes of the Apennines and central Italy coastal areas. These events are favoured by intense air-sea interactions and it is reasonable to hypothesize that the Adriatic Sea surface temperature (SST) can affect the amount and location of precipitation.

High-resolution simulations of different Bora and Sirocco events leading to severe precipitation are performed using a convection-permitting model (MOLOCH). Sensitivity experiments varying the SST initialization field are performed with the aim of evaluating the impact of SST uncertainty on precipitation forecasts, which is a relevant topic for operational weather predictions, especially at local scales. Moreover, diagnostic tools to compute water vapour fluxes across the Italian coast and atmospheric water budget over the Adriatic Sea have been developed and applied in order to characterize the air mass that feeds the precipitating systems. Finally, the investigation of the processes through which the SST influences location and intensity of heavy precipitation allows to gain a better understanding on mechanisms conducive to severe weather in the Mediterranean area and in the Adriatic basin in particular.

Results show that the effect of the Adriatic SST (uncertainty) on precipitation is complex and can vary considerably among different events. For both Bora and Sirocco events, SST does not influence markedly the atmospheric water budget or the degree of moistening of air that flows over the Adriatic Sea. SST mainly affects the stability of the atmospheric boundary layer, thus influencing the flow dynamics and the orographic flow regime, and in turn, the precipitation pattern.

Highlights

- Numerical simulations of heavy precipitation associated with intense air-sea interaction over the Adriatic Sea.
- Sensitivity of forecast precipitation to SST uncertainty.
- The response of intense precipitation patterns to SST uncertainties is complex.
- SST impact on dynamics and on orographic flow regime and, in turn, on precipitation.

Keywords:

Heavy precipitation; SST; air-sea interaction; orography; water budget

1. Introduction

The Adriatic basin is characterized by a shallow and semi enclosed sea surrounded by orography on both the western (Apennines) and the eastern (Dinaric Alps) sides, as well as to the north (Alps). This morphology plays a key role in favouring severe weather events over Italy, in particular those associated with the interaction between orography and two types of intense low-level flow over the Adriatic Sea, namely moist southeasterly flow (typically referred to as Sirocco) and cold and relatively dry gusty northeasterly flow (Bora). Specifically, Sirocco wind impinges on the Alpine reliefs and makes northeastern Italy (NEI) an area prone to heavy precipitation, floods and storm surges (De Zolt et al., 2006; Borga et al., 2007; Davolio et al., 2009; Barbi et al., 2012; Manzato et al., 2015, Davolio et al., 2016). Bora wind jets impinge on the complex coastal orography of the Apennines reliefs, exposing the northern and central regions of Italy to strong winds, heavy precipitation, including snowfall, and severe storm surges and floods along the coast (Grazzini, 2013; Ferretti et al., 2014; Maiello et al., 2016).

Although Bora and Sirocco display different characteristics, they are both associated with intense air-sea exchange of heat, momentum and humidity, and differences between air and sea surface temperature (SST), together with intense winds, are responsible for a remarkable enhancement of heat and moisture fluxes at the sea surface (Pullen et al., 2006; Dorman et al., 2007; Raicich et al., 2013; Davolio et al., 2015; Ricchi et al., 2016). The consequence of intense air-sea interaction in terms of its capacity to lead to heavy precipitation events is a topic still under discussion and that has been receiving lot of attention (Ludwig et al., 2014; Rainaud et al., 2016; Stocchi and Davolio, 2016). Recent studies (Ferretti et al., 2014; Manzato et al., 2015; Davolio et al., 2016; Davolio et al., 2017), described the thermodynamic mechanisms leading to intense rainfall in the Adriatic basin, identifying also air-sea exchange as a key aspect to be considered. Whether characterized by orographic (stratiform or convective) precipitation over the Alpine/Apennines slopes or over the plain region between the sea and the mountain ranges, it is reasonable to hypothesize that the amount of heat and moisture gained from the Adriatic Sea and transported by Sirocco and Bora wind can have an impact on severe weather events. In fact, surface fluxes contribute to increase atmospheric moisture content and to determine the characteristic of the low-level flow and especially its stability. This in turn could influence the orographic flow regimes (Smith, 1979) and thus the location, intensity and characteristics of the precipitation (Cassola et al., 2016; Davolio et al., 2017).

Several studies in the last decade focused on the analysis of the interaction between the sea and the atmosphere and in particular on its impact on heavy rain (e.g. Rainaud et al., 2016). All these

studies pointed out the important role of SST, which influences turbulent heat and water vapour surface fluxes (e.g. Dorman et al., 2007; Pullen et al., 2007). In the tropics the relationship between SST and atmospheric phenomena is well known. In this area higher SST are generally accompanied by enhanced convective activity and precipitation (Trenberth and Shea, 2005). Roxy and Tanimoto (2012) found that positive SST anomalies induce unstable conditions in the lower atmosphere and enhance the precipitation anomalies. Toy and Johnson (2014) highlighted that even mesoscale SST fronts influence the PBL stability, resulting in increased horizontal convergence and precipitation. On the other hand, at mid-latitudes and in the Mediterranean basin in particular, the impact of SST on severe weather events is still debatable and different recent studies tried to address this issue for different atmospheric phenomena. For instance, the effect of SST has been recently evaluated for the development of Mediterranean tropical-like cyclones (Miglietta et al., 2011; Romaniello et al., 2015), for deep cyclones in the Eastern Mediterranean (Katsafados et al., 2011), for mid-latitude storms (Booth et al., 2012) and for heavy precipitation (Meredith et al., 2015; Pastor et al., 2015). Concerning intense rainfall, Pastor et al. (2001), using a high-resolution non-hydrostatic model, showed significant improvements in the peak precipitation forecasts using a SST derived from NOAA satellite data. Lebeaupin et al. (2006) examined the influence of SST on short-range forecasts of torrential rain events that occurred over southeastern France. They showed that variations of SST by several degrees on average and on a large enough area have a noticeable influence on surfaces fluxes, on PBL stability and on the intensity of convective systems, while small-scale SST patterns, as those produced by the use of high-resolution SST products, are not of primary importance. Cassola et al. (2016), found a positive impact of high-resolution SST analyses for heavy precipitation forecasts over Liguria (Italy), except in the short-range when it is generally neutral or even negative. Senatore et al. (2014) obtained contrasting results concerning the effect of SST on simulations of intense rain events in southern Italy. Finally, on longer time-scale, Berthou et al. (2014, 2015), using a coupled atmospheric-ocean modelling system, showed that intense rain events in the Cévennes region are mainly sensitive to the long-term change of SST, with a smaller but significant contribution of rapid events. Moreover, analysing 30 extreme precipitation events over the whole Mediterranean basin, Berthou et al. (2016) showed a relation between rainfall and SST in the upstream area mainly ascribable to modification in low-level dynamics rather than in low-level specific humidity.

All these studies indicate a vivid interest in the subject but they also suggest that although an intense rain event can be sensitive to SST definition and evolution, the response is always complex and hardly systematic. Moreover, regarding the Adriatic area, evidences on the role of SST on heavy rain have not been clearly showed yet. Therefore, the role of SST deserves further

investigations, especially considering that SST fields (from global analyses or satellite estimates), used to initialize numerical weather prediction (NWP) forecasts, can be affected by significant uncertainties and sometimes display relevant differences among each other, even of the order of some degrees during particular intense events like Bora (Davolio et al., 2015). Moreover, NWP models, applied to short-range forecasts, often keep SST fixed at its initial value or allow just slow changes according to surface fluxes during the integration. Some recent studies in this area (Tudor et al., 2015; Davolio et al., 2015; Ricchi et al., 2016), although not focusing specifically on heavy precipitation, showed that an accurate Adriatic SST initialization and evolution is critical for a correct description of an exceptional Bora wind event, and that SST analysis can be affected by remarkable errors, especially in small and shallow basin like the Adriatic Sea.

The purpose of the present study is thus to better understand the influence of the Adriatic SST uncertainty on the physical processes (dynamics, surface fluxes, water budget) leading to heavy precipitation events associated with intense Sirocco and Bora winds, thus with intense air-sea interactions. To attain this aim, sensitivity experiments using a high-resolution NWP model were performed. This work may be viewed as an extension and a completion of a preliminary study by Stocchi and Davolio (2016) that has already analysed three Sirocco events showing a complex effect of the Adriatic SST on precipitation. Here a more detailed analysis of Sirocco cases is performed, even extended to Bora events, thus complementing previous preliminary results. Also, a specific tool aimed at evaluating water budget in the atmosphere over the Adriatic Sea has been developed and applied, together with the computation of vertical profiles and vertically integrated water vapour fluxes. This allows to characterize the air masses feeding the precipitation systems and to describe the low-level flow interaction with the orography.

The paper is organized as follows. The NWP system and its specific implementation for the present research activity are described in Section 2. An overview of the selected case studies is presented in Section 3 and 4. Section 5 describes atmospheric water balances and vertically integrated water vapour fluxes analysis. Section 6 presents the main findings concerning involved physical mechanisms and dynamics. Finally conclusions are drawn in Section 7.

2. Numerical models: description and set up

The NWP system employed for the simulation is based on the hydrostatic BOLAM and non-hydrostatic MOLOCH models, developed by the Institute of Atmospheric Sciences and Climate of the Italian National Research Council (CNR-ISAC). This NWP system is used operationally at

147 various Italian national agencies and regional meteorological services and it is also used
148 operationally at ISAC as part of an agreement with the National Civil Protection Department.
149 BOLAM and MOLOCH limited area models differ mainly in the dynamical core, in the vertical
150 coordinate discretization, and by the fact that BOLAM includes the Kain–Fritsch scheme – using a
151 modified version based on Kain (2004) – to parameterize convection, while in MOLOCH, deep
152 convection is explicitly simulated and a simple shallow convection scheme is applied. However,
153 atmospheric radiation, atmospheric boundary layer and surface layer parameterizations, soil
154 processes and, to a large extent, microphysical processes are common in the two models.
155 In the present study, initial and boundary conditions for BOLAM are provided every 3 hours by
156 IFS-ECMWF forecasts and thus the SST initial field is derived by the OSTIA analyses (Donlon et
157 al., 2012). BOLAM runs over a European domain (shown in Fig. 1a), with a horizontal resolution of
158 about 11 km, 418 x 290 grid points and 50 vertical levels. BOLAM is mainly employed to provide
159 lateral boundary conditions at 1-hour intervals to the inner grid of MOLOCH. MOLOCH
160 integration domains are shown in Fig. 1b (354 x 322 grid points) and in Fig. 4a (514 x 514 grid
161 points) for Sirocco and Bora events simulations, respectively. MOLOCH is initialized with a 3-hour
162 BOLAM forecast in order to avoid a sudden change in the grid resolution from the global model to
163 the 2.2 km MOLOCH grid-spacing, based on pure interpolation. Since the results discussed here are
164 based mainly on MOLOCH simulations, only a brief and general description of MOLOCH is
165 provided in the following. For a description of BOLAM see Buzzi et al. (2003) and Malguzzi et al.
166 (2006).
167 MOLOCH is a non-hydrostatic, fully compressible, convection-permitting model (Malguzzi et al.,
168 2006; Buzzi et al., 2014). It integrates the set of atmospheric equations with 12 prognostic variables,
169 pressure, absolute temperature, specific humidity, horizontal and vertical components of velocity,
170 turbulent kinetic energy and five water species (cloud water, cloud ice, rain, graupel and snow)
171 represented on the latitude–longitude, rotated Arakawa C-grid. It employs a hybrid terrain-
172 following vertical coordinate (50 vertical levels in this application, lowest level at 70 m above the
173 surface), depending on air density and smoothing to horizontal surfaces at higher altitudes. Time
174 integration is based on an implicit scheme for the vertical propagation of sound waves, while
175 explicit time-splitting schemes are implemented for integration of the remaining terms of the
176 equations of motion. Three-dimensional advection is computed using the Eulerian weighted average
177 flux scheme (Billet and Toro, 1997). The microphysical scheme is based on the parameterization
178 proposed by Drofa and Malguzzi (2004). Atmospheric radiation is computed with a combined
179 application of the Ritter and Geleyn (1992) scheme and the ECMWF scheme (Morcrette et al.,
180 2008). The turbulence scheme is based on a turbulent kinetic energy−mixing length (E−l) order 1.5

closure theory (Zampieri et al., 2005). The soil model uses seven layers and it takes into account the observed geographical distribution of different soil types, vegetation coverage and soil physical parameters. In particular, the evolution of SST is computed by a simple slab ocean model, in which the deep ocean temperature is kept fixed, while SST evolves in the surface layer depending on radiative and latent/sensible heat fluxes. The surface layer is a few metres deep, and its thickness may vary as a function of the wind intensity. The initial analysed distribution of SST is used as a relaxation reference value (relaxation time of about 2 days), thus allowing a smooth transition toward the deep ocean.

In order to cover as much as possible different types of events and periods of the year, the NWP system was applied to simulate three Bora and three Sirocco cases (Table 1). First, a verification of the simulations against available observations was performed in order to assess that the model correctly reproduced the main dynamical features and precipitation patterns of each event. Then, in order to evaluate the influence of SST uncertainty on precipitation forecasts and to investigate the physical processes involved, sensitivity tests were carried out for each event, modifying the initial value of SST (used in the reference CNTRL simulation) over the Adriatic Sea by +2°C (experiment SST2P) or -2°C (SST2M). These values can be considered reasonably representative of the uncertainty associated with SST operational analysis, as shown in previous studies (e. g. Lebeaupin et al., 2006; Davolio et al., 2015). The model chain is initialized at least 12 hours before the onset of intense rainfall, in order to allow the PBL to adjust to the modified SST initial field.

3. Sirocco events and simulation results

The direct orographic uplift of the southerly moisture-laden flow from the Adriatic Sea is often responsible for long-lasting orographic precipitation in the NEI Pre-Alpine and Alpine areas. In case of conditionally unstable flow, the interaction with the orography may lead to the formation of intense convective system upstream of the orography (Barbi et al., 2012; Manzato et al., 2015; Davolio et al. 2016). In the present study, the three analysed events occurred under similar synoptic conditions (Fig. 1a), characterized by an approaching upper-level trough extending over the Mediterranean, associated with an intense low-level southeasterly flow (Fig. 1b) over the Adriatic Sea (Sirocco). However, the three events presented quite different precipitation characteristics (Table 1), due to the different season and the different thermodynamic properties of the impinging flow. In particular SIR-03 event (Fig. 2c) occurred in late summer (14 - 16 September 2006) and was characterized by a marked convective activity, with precipitation systems affecting also the plain area close to the Adriatic coast. On the other hand, the other two cases, SIR-01 (Fig. 2a) and

SIR-02 (Fig. 2b) occurred in autumn, on 10 - 12 November 2012 and 30 October - 2 November 2010, respectively, and were characterized mainly by stratiform orographic rainfall (more details in Davolio et al., 2016). The results of the SST sensitivity tests were already discussed in Stocchi and Davolio (2016) and just a brief summary is provided in the following.

3.1 SIR-01

Between 10 and 11 November 2012, an upper level trough deepening over the Iberian peninsula and northern Africa (Fig. 1a) activated intense warm and moist southwesterly flow over the central Mediterranean. The trough moved slowly eastward, eventually evolving into a cut-off low over Spain. Heavy rainfall (almost 400 mm in 24 hours), sustained by the moist low-level flow over the Adriatic Sea (Fig. 1b), affected the Pre-Alpine area (Fig. 2a) between Veneto and Friuli Venezia Giulia (FVG) regions, while weak precipitation was recorded over the plain.

MOLOCH correctly predicts the orographic precipitation. However, the maximum accumulation is slightly underestimated: 310 instead of 390 mm in 24 hours at Piancavallo, over the FVG Alps. The different SST initialization (SIR-01-SST2P, SIR-01-SST2M) produces relevant displacements of rainfall location (Figs. 3a, b): a colder (warmer) SST is associated with upstream (downstream) displacement of the intense precipitation area with respect to the Alpine orography. Moreover, in SIR-01-SST2M intense rainfall is also displaced over the plain and affects a large portion of the Po Valley (more details in Stocchi and Davolio, 2016).

3.2 SIR-02

As in SIR-01 event, in SIR-02 rainfall was associated with a deep trough over the Mediterranean basin, evolving into a cut-off low over the Gulf of Lion, and with intense low-level Sirocco wind over the Adriatic Sea. The eastward movement of the trough was slowed by the presence of a pressure ridge over Eastern Europe progressively reinforcing, thus favouring the persistence of precipitation over the same Alpine area. Intense rainfall distribution resulted strictly correlated with orographic features along a WSW–ENE direction over the Pre-Alps (Fig. 2b) and the pattern did not change during 31 October and 1 November. Heavy rainfall reached 460 mm in 48 hours in Veneto and about 600 mm in 48 hours in FVG (Davolio et al., 2016).

Contrary to SIR-01, in SIR-02 event the impact of the different SST initialization (SIR-02-SST2P and SIR-02-SST2M) produces just rather small displacements of rainfall location (Figs. 3c, d).

3.3 SIR-03

During 14 September 2006, an upper level trough deepened over the western Mediterranean. While

moving slowly eastward, it was responsible for the development of a cyclonic circulation in the lower troposphere characterized by a pressure minima located between southern France and Corsica on 15 September. This synoptic pattern favoured intense Sirocco over the Adriatic basin. Due to the unstable vertical profile, the southeasterly low-level flow triggered convective activity over the sea, over the Italian coastal area and over NEI plain. However, rainfall reached maximum intensity over FVG orography (almost 300 mm in 24 hours), directly exposed to the impinging moist currents. As in SIR-01, in SIR-03 the impact of SST is relevant (Figs. 3e, f). SIR-03-SST2M is generally dryer than SIR-03-CNTRL, while a warmer SST (SIR-03-SST2P) produces a shift of the rainfall towards the northern Adriatic coast and towards the eastern part of the domain.

As discussed in Stocchi and Davolio (2016), the response to different SST seems complex. SST does not affect directly precipitation by modifying the amount of water vapour that impinges on the Alps. Instead, SST plays mainly an indirect role (as will be further discussed in the next sections), since it determines the boundary layer (PBL) thermodynamic structure, which in turn affects the flow dynamics and its interaction with the orography.

4. Bora events and simulation results

Bora wind frequently affects the Adriatic basin especially during the cold season. Long-lasting events are characterized by intense air-sea interaction and they are often associated with heavy precipitation that affects the northern and central regions of Italy particularly exposed to northeasterly currents impinging on the Apennines.

Three events are selected and analysed in this study (Table 1) in order to cover as much as possible different types of Bora (cyclonic and anticylonic Bora, Horvath et al., 2009) that produced relevant effects in terms of precipitation over Italy, in particular over the Apennines slopes, in different periods of the year. Two of them are cyclonic Bora events, BOR-01 (9 - 11 February 2012) and BOR-02 (13 - 15 September 2012, Fig. 4a), and one is an anticyclonic Bora event, BOR-03 (30 - 31 December 2014, Fig. 4b). They are all long-lasting episodes, characterized by at least 48 hours of strong northeasterly flow.

It is worth mentioning that in the two winter events precipitation was mostly snowfall, and raingauge measurements were affected by a relevant underestimation. Therefore, reliable observed precipitation maps are not available. MOLOCH forecast validation was not straightforward and it was performed using a subset of significant weather stations for which data have been quality-controlled, as well as comparing model results against technical reports and data (including snow depth) from Regional Meteorological Services (as described in details in Henin, 2015, Davolio et

al., 2017 and reference therein). Moreover, a validation of model forecasts for the exceptional Bora case of February 2012 (BOR-01) was recently undertaken (Davolio et al., 2015).
Only a brief description of the selected events is provided in the following and model simulation results are presented.

4.1 BOR-01

BOR-01 event is part of an exceptionally severe Bora episode, which lasted for almost twenty days (Raicich et al., 2013; Mihanović et al., 2013; Grazzini 2013) and produced important effects also on the Adriatic Sea circulation (Benetazzo et al., 2014). By the end of January 2012, the synoptic situation over Europe was dominated by a blocking configuration characterized by a pressure ridge meridionally elongated over the eastern Atlantic. This configuration determined a prevailing meridional circulation over Europe and favoured the descent of cold continental air towards the Mediterranean. Until mid-February, the Mediterranean basin was characterized by a persistent cyclonic circulation associated with an exceptionally cold anomaly. This pattern produced heavy precipitation over northern and central Italy, as well as persistent and strong Bora wind over the Adriatic Sea. In this study we focus our attention on the period between 10 and 12 February when precipitation reached its most intense phase (even exceeding 120 mm in 48 hours both over northern and central Apennine) and exceptional snowfall occurred along the foothill of the Apennines exposed to northeasterly winds. In the following a description of the modelling results is provided.
MOLOCH simulation (BOR-01-CNTRL) correctly forecasts the two distinct area of heavy precipitation over the northern and central Apennines regions, with almost 100 mm in 24 hours (Fig. 5a). Over the central Adriatic Sea, a wide band of intense precipitation is observed from radar (not shown) and correctly simulated, extending from southeast to northwest towards the Italian coast. This band corresponds with a region of convergence between the southernmost Bora jet and a warmer southeasterly low-level flow associated with the cyclonic circulation (Fig. 6a).
When the Adriatic SST is modified in the sensitivity experiments, the precipitation pattern presents a different distribution. Figure 7 shows the difference among daily-accumulated precipitation of BOR-01-CNTRL simulation and the simulations with modified SST (BOR-01-SST2P and BOR-01-SST2M). Red colour indicates areas where the CNTRL run is more rainy. A colder SST produces a slight decrease of the intensity of the northern precipitation maximum and a clear shift to the south of the rainfall area over central Italy (Fig. 7a). Conversely, the effect of a warmer SST is to slightly increase the precipitation over the northern Apennines and to displace to the north the precipitation pattern over central Italy (Fig. 7b). The wind field in the lower troposphere (Fig. 6) shows that the

region of convergence (over the sea, around 43 N) between the southernmost Bora jet and the warmer southeasterly wind is displaced consistently. While the position of the Mediterranean cyclone, close to the western Italian coast, remains unchanged, in BOR-01-SST2P (Fig. 6c) the moist southerly low-level wind penetrates more to the north over the Adriatic basin. Contrarily, in BOR-01-SST2M the southerly cyclonic wind is confined more to the south by the presence of a more intense Bora jet. The different interaction between Bora and southeasterly cyclonic flow, due to different SST, is responsible for the different precipitation patterns. Understanding how the SST affects this interaction and its impact on surface fluxes is therefore essential and requires a more detailed analysis that will be provided in Sections 5 and 6.

4.2 BOR-02

After a prolonged warm and moist period that produced high temperature and humidity values over Italy, by 12 September 2012 a large-scale through moved from Scandinavia towards Germany and northern Italy. The associated cold front passed over the Alps and a lee cyclone (Buzzi and Tibaldi, 1978) formed over the Tyrrhenian Sea on 13 September (Fig. 4a). The slow southerly movements of the cyclone favoured a prolonged period of Bora wind over the Adriatic Sea, with persistent orographic and convective rainfall affecting the central Italy area (Fig. 5b). It is worth noting that this event occurred during the first field campaign (SOP1) of the Hydrological Cycle of the Mediterranean Experiment (HyMeX) programme (Ducrocq et al., 2014) and thus it was extensively monitored (Ferretti et al., 2014).

The reference simulation (BOR-02-CNTRL) succeeds in reproducing the observed precipitation field (see Fig. 2 in Maiello et al., 2016), in terms of both intensity and distribution with only a slight underestimation of some local maxima (Fig. 5b). Specifically four distinct rainfall peaks quite close to each other over central Italy, with intensities between 130 and 290 mm in 24 hours, are well reproduced over an area approximately enclosed between Marche and Abruzzo regions.

Differences between daily-accumulated precipitation fields of BOR-02-CNTRL simulation and of BOR-02-SST2P and BOR-02-SST2M experiments (Figs. 7c, d) underline that colder (warmer) SST produces a weaker (stronger) pattern of rainfall, slightly displaced upstream (downstream) with respect to the orography. Figure 8 reveals different characteristics of the low-level wind. Colder SST (BOR-02-SST2M) produces less intense Bora jets, which propagate to a smaller distance inland of the Italian coast (Fig. 8b). The wind associated with the southernmost Bora jet is almost blocked by the presence of the Apennines and even deflected to the south along the coast. Warmer SST (BOR-02-SST2P) produces a more intense Bora (Fig. 8c), and the wind is able to flow over the orography of the central Apennines. The modification of the orographic flow regime in these

experiments seems responsible for the differences in the precipitation fields showed in Figs. 7c, d.

4.3 BOR-03

By 30 December 2014, the synoptic circulation was characterized by the presence of a high-pressure ridge extended meridionally along the European Atlantic coast, progressively turning its axis while expanding north of the Alps and over Central Europe at all levels (Fig. 4b). The strong pressure gradient drove cold air from continental Eurasia towards the Dinaric Alps, flowing across the southern edge of the ridge, thus producing intense Bora over the Adriatic Sea, in particular over the central and meridional part of the basin. As typical of anticylonic Bora events, the wind was northeasterly all along the vertical profile, since anticyclonic Bora is usually much deeper and weaker than cyclonic one (Göhm and Mayr, 2005). This case was not particularly severe in terms of precipitation, but it affected the entire Adriatic (the most intense Bora jet blew in correspondence to the southern Dinaric gaps), producing a quite exceptional snowfall over the Italian coastal areas. The precipitation pattern organized along narrow bands starting from the coast and aligned with the low-level wind streaks (Fig. 5c) with a localized maximum inland over central Italy (70 mm/24h, not shown).

BOR-03-CNTRL simulation is able to reproduce the main peaks, but forecasts the precipitation mainly inland, over the Apennines reliefs, where Bora wind directly impinges (Fig. 5c). The precipitation differences between BOR-03-CNTRL, BOR-03-SST2M and BOR-03-SST2P for this event (Fig. 7e, f) show just rather small displacements of the precipitation, without a critical direct or indirect impact of the Adriatic SST.

5. Water vapour profile and water balance in the atmosphere

The sensitivity experiments indicate that SST affects precipitation and the wind pattern of Sirocco and Bora over the Adriatic Sea and inland. SST changes could affect the precipitation directly, increasing or decreasing the evaporation from the Adriatic Sea, or indirectly modifying the PBL thermodynamic characteristics and consequently the flow dynamics and its interaction with orography. In order to better understand the role of SST on different processes relevant for heavy precipitation, some diagnostic tools were developed and applied. Results will be discussed in the following sections. This aspect was only preliminarily and partially tackled in Stocchi and Davolio (2016) for Sirocco cases, with the analysis of vertically integrated water vapour fluxes. Here, it is complemented with the computation of the atmospheric water budget over the Adriatic Sea and extended to Bora events.

385

386 **5.1 Analysis of Sirocco events**

387 Vertically integrated water vapour fluxes (IWVF), as in Manzato (2007), Duffourg and Ducrocq
388 (2011) and Davolio et al. (2017), were computed along the Adriatic coastline (see Fig. 3 in Stocchi
389 and Davolio, 2016) in order to evaluate the influence of SST changes on the total amount of water
390 vapour transported by the low-level flow (up to 3000 m) towards the Alps and feeding the
391 precipitation system. Results showed that a different SST does not modify systematically the
392 amount of moisture moving inland. In particular, IWVF are just slightly modified or even
393 unaffected by changing SST for SIR-01 and SIR-02, respectively, while for SIR-03, an increase of
394 SST produces an evident eastward shift of the main moisture advection across the northern Adriatic
395 coastline, as the wind field is also modified (as will be shown in detail in Section 6).
396 The computation of IWVF does not provide information about the sources of moisture and does not
397 allow to quantify the importance of surface fluxes, and the possible impact of SST, with respect to
398 the transport of moisture due to large scale circulation. Therefore, in order to compute a water
399 budget analysis inside a defined volume of atmosphere over the Adriatic Sea, a 3d-rectangular box
400 (Fig. 1b) is arranged as to cover the area affected by the low-level Sirocco flow. Its bottom face is
401 attached to the sea surface and the top face is in the troposphere. The northern side of the box is
402 placed in correspondence of the northern Adriatic coast, just upstream of the area affected by
403 intense rainfall, and together with the southern face it is aligned in order to intercept the prevailing
404 southeasterly flow, feeding the precipitation system. The water budget analysis tool computes
405 evaporation and precipitation at the bottom side, advection of vapour and hydrometeors (solid and
406 liquid components of clouds and precipitation) across the four lateral sides and the top. The box
407 balance is computed hourly and converted into energy units (Watts). A more detailed description of
408 the water budget computations is provided in Davolio et al. (2017). It is worth saying that results do
409 not depend significantly on the box design, in particular on its meridional extension, as verified
410 with sensitivity tests.
411 First, the closure of the balance was verified by placing the top of the box at 20 km, as in Duffourg
412 and Ducrocq (2013), thus assuming that the contribution to total fluxes of water at the top were
413 negligible, and comparing all the mentioned contributions with the tendency of the Integrated Water
414 Vapour inside the box (computed considering all the atmospheric water species). A satisfactory
415 agreement is found, with only some negligible discrepancies, probably ascribable to the comparison
416 of instantaneous hourly values on lateral sections with integral values at the bottom, as well as to
417 numerical inaccuracies due to interpolation of the variables on the sections. Then the budget was
418 computed for boxes with top at different elevation in order to highlight the contribution associated

with the low-level flow and the role of surface fluxes (results for 3-km high boxes are shown).

The evolution in time of the water budget terms for each side of the box (negative values always indicate outflow from the box) is displayed in Fig. 9 for the three CNTRL simulations. The contribution through each side of the box is displayed together with upward fluxes from the Adriatic Sea. For all the events, the contribution associated with the Sirocco is evident, with inflow (outflow) from the southern (northern) face attaining maximum values around $1.0 \cdot 10^{14}$ W. The contribution of the western section becomes more relevant as the height of the box increases, due to the typical veering of the wind at higher elevation. For 3-km high boxes, it is comparable or even higher (as for SIR-01 and SIR-02 events) than that of the southern section. Outflow from the northern section (and partially also form the eastern one) is supposed to directly contribute to the precipitation downstream. It is worth noting that the bottom term of the Adriatic box is by far the least important ($0.1 \cdot 10^{14}$ W) with a negligible contribution to the water supply.

The water budget analysis for SST2P and SST2M (not shown) exhibits similar pattern, with negligible differences in the values of lateral terms, and still a very modest contribution of the evaporation to the total water budget.

These results underline that the Adriatic SST does not influence markedly the atmospheric water budget available for precipitation, since it is dominated by mesoscale transport, while the amount of moisture that enriches the airmass humidity during its passage over the sea is almost negligible. It follows that the influence of the SST on heavy precipitation in the three analysed Sirocco cases can be explained through dynamical processes (see Section 6) and not as a consequence of a direct effect on the water mass-balance.

5.2 Analysis of Bora events

5.2.1 Water vapour profile

For the Bora events, the IWVF are computed across a vertical section aligned along the Italian Adriatic coast, up to 3000 m, in order to analyse the amount of moisture moving from the Adriatic towards the Apennines, where most of the precipitation occurs. The IWVF are computed for each model grid point corresponding to the Italian coastline (Fig. 10) from about 42.2 N to 45.5 N.

For BOR-01-CNTRL simulation, the IWVF maximum value (180 $kg \cdot m^{-3}$) is associated with the most intense Bora jet reaching the Italian coast at a latitude between 42.5 N and 43.0 N. This corresponds also to the area where the southeasterly flow associated with the cyclonic circulation converges with Bora (Fig. 6) and where the maximum of precipitation is observed inland (Fig. 5a). BOR-02-CNTRL simulation produces a similar IWVF pattern, but with a higher maximum value

(380 kg·m^{-3}). This is consistent with a much higher amount of precipitation over the Apennines (Fig. 5b) for this event. In both cases, the abrupt decrease of IWVF south of 42.5 N is due to the fact that the wind becomes almost aligned with the coastline. Finally, BOR-03-CNTRL event produces an IWVF pattern that reveals the presence of several low-level jets and thus a more uniform distribution of the peaks intensity all along the Italian coast.

For all the three events, IWVF values simulated in CNTRL are compared with IWVF values obtained in the SST2P and SST2M experiments (Fig. 10). As observed for the Sirocco events, also in case of Bora the SST changes do not markedly modify the IWVF, that is the amount of water vapour transported inland by the low-level wind. For BOR-01 case, the differences in IWVF among the experiments are mainly in terms of displacement of the peaks along the coast. In fact, the location where the maximum IWVF value is attained is shifted to the north (south) in BOR-01-SST2P (BOR-01-SST2M) case, consistently with the displacement of precipitation and of the convergence line described in the previous section.

For BOR-02, and to a lesser extent also for BOR-03 case, experiment SST2M produces a slight reduction of the IWVF maximum, consistently with the decrease in Bora intensity and in precipitation described in the previous section. However, this suggests also a possible direct role of the SST on low-level moisture amount, which is eventually responsible for orographic precipitation over the Apennines. An evaluation of the atmospheric water balance over the Adriatic Sea is carried out in the following section to gain a deeper understanding concerning the role of the SST in heavy precipitation events associated with intense and persistent Bora.

5.2.2 Water balance in the atmosphere

For the three Bora cases, the same procedure described in Section 5.1 is adopted, but a different 3d-rectangular box is employed (as shown in Fig. 8c). Here, the eastern and western sides are aligned almost parallel to the mountain ranges, namely the Dinaric Alps and the Apennines, intercepting the Bora wind flow almost orthogonally, while the northern and southern sides are consequently placed across the Adriatic Sea. First the closure of the balance is verified; then the budget is computed for a box with top at 3 km.

The water balance for BOR-01 case (Fig. 11a) is dominated by the contribution of advection through the eastern and western sections due to Bora, with maximum values of about $0.8 \cdot 10^{14}$ W and $-0.8 \cdot 10^{-14}$ W, respectively. The contribution across the southern face becomes relevant only at a later stage of the event (up to $0.4 \cdot 10^{-14}$ W) as a consequence of the intensification of cyclonic circulation, which conveys water from the south and the southeast into the box in the middle-lower

troposphere. Finally, the bottom term of the Adriatic box is by far smaller ($0.1 \cdot 10^{-14}$) than lateral advection, providing a negligible contribution to the budget.

A similar balance characterizes BOR-02 event (Fig. 11b), although with much higher values, exceeding $2.0 \cdot 10^{14}$ W and $-2 \cdot 10^{14}$ W at the western and eastern sections, respectively, as a consequence of the higher temperature and water content in that period (early autumn) of the year. The magnitude of southern component and the northern component is almost unchanged with respect to the previous event, and the contribution from the bottom is still negligible.

Conversely, a different balance characterizes BOR-03 event (Fig. 11c). Advection across the western section ($-0.7 \cdot 10^{14}$ W), which is supposed to directly contribute to the precipitation, still dominates the outgoing portion of the balance, and it is essentially compensated by the sum of the inflow through the eastern side ($0.4 \cdot 10^{14}$ W) and the evaporation from the sea surface ($0.2 \cdot 10^{14}$ W). It is interesting to note that in general, all the horizontal transport (advection) terms present significantly lower values than those attained in the two previous cyclonic Bora cases. Therefore, in this situation, the contribution of the sea surface fluxes to the water budget becomes more relevant, although the magnitude of Adriatic surface flux is only slightly higher than in the cases of cyclonic Bora (Table 1). Both northern and southern sections contributions are almost negligible, due to a northeasterly wind which blows uniformly at all levels and all over the Adriatic basin (as expected in case of anticyclonic Bora).

As for the Sirocco cases, the water budget analysis for SST2P and SST2M experiments for all the three Bora cases (not shown) provides results similar to the CNTRL runs, with just some negligible differences. Therefore, this analysis indicates that also for Bora events the SST does not influence markedly the atmospheric water budget, which is still dominated by the mesoscale transport. Once more, the analyses of IWVF and of the water budget indicate that the influence of SST on heavy precipitation is complex and it is not ascribable solely to a modification of moisture supply from the surface. In case of intense air-sea interaction, the response of precipitation to SST probably involves a modification of the dynamics of low-level winds.

6. Influence on dynamics and interaction with orography

The analysis of the atmospheric water budget pointed out a limited contribution due to evaporation from the Adriatic Sea, except to some extent for the anticyclonic Bora event (BOR-03) occurred in December 2014. Consequently, the variations of +/-2 °C of SST applied over the Adriatic in the sensitivity experiments do not modify significantly the balance. However, SST clearly influences precipitation amount and location as well as the wind field. Therefore the effect of SST on the

520 dynamics needs to be investigated.
521
522 **6.1 Sirocco cases**
523 The preliminary dynamical analysis presented in Stocchi and Davolio (2016) for the Sirocco events
524 showed that the SST plays an indirect role in determining the location of rainfall, influencing the
525 PBL characteristics and consequently the low-level wind and its interaction with the orography.
526 Here the purpose is to identify the relevant dynamical processes, associated with SST changes; to
527 attain this aim meteorological variables are analysed over vertical sections (see Fig. 1b for their
528 location).
529 Figure 12 shows potential temperature and tangent wind component over the section drawn just
530 upstream (and parallel to) the Alpine chain (section d1 shown in Fig. 1b), for the SIR-01 case at
531 0900 UTC, 11 November 2012. In the SIR-01-CNTRL experiment (Fig. 12a), cold air is present
532 over NEI plain areas and at the foothills of the eastern Alps, from the surface up to 1000 m. Winds
533 are more intense over the eastern part of the Alps, and gradually decrease in intensity moving to
534 southwest over the plain. Just upstream the Alpine chain, the section shows a shallow layer of
535 relatively cold air flowing towards southwest, parallel to the Alps. As described in Davolio et al.
536 (2016) this is due to southeasterly low-level wind blocked and deflected by the orography, resulting
537 in a northeasterly barrier wind. In SIR-01-SST2M (Fig. 12b), the low-level northeasterly barrier
538 wind is more intense and blows parallel to the Alps all along the section. Potential temperature in
539 the lower troposphere is colder and a stronger vertical stratification is produced with respect to SIR-
540 01-CNTRL, especially over the plain. The intensity of the vertical motion over the orography is
541 markedly reduced. Conversely, in SIR-01-SST2P, air in the lower troposphere is warmer and
542 characterized by more intense vertical motions over the orography. It is worth noting that the low-
543 level wind in the western portion of the section is not deflected anymore over the plain by the
544 orography, since it is able to entirely flow over the Alps.
545 Therefore, changes of SST influence the thermodynamic structure of the PBL even downstream of
546 the sea, over northeastern Italy plain, thus modifying the dynamical behaviour of the Sirocco flow
547 impinging on the orography. This determines a transition from blocked-flow in SIR-01-SST2M to
548 flow over in SIR-01-SST2P. In SIR-01-SST2M, the deflection of the low-level flow from the
549 Adriatic Sea, due to orographic blocking, is responsible for a larger precipitation amount over the
550 Po Valley (Fig. 3a) and an upstream shift of the rainfall pattern with respect to the Alps. In SIR-01-
551 SST2P, where the warmer and more buoyant impinging flow is able to rise over the orography, the
552 precipitation pattern is shifted downstream compared to SIR-01-CNTRL. This result is confirmed
553 by the cross sections (section d2, shown in Fig. 1b) drawn along the direction of the Sirocco wind

554 and showing cloud water/ice content and vertical velocity (Fig. 13). The effect of increasing SST is
555 to intensify the vertical motions and to shift downstream, towards the mountain crest, the area with
556 intense orographic uplift and condensation.
557 Also in SIR-03 case (Fig. 14) the SST effect is relevant, because it determines the interaction
558 between the Sirocco over the Adriatic and the southwesterly flow descending from the northern
559 Apennines as a dry föhn-like wind. In SIR-03-SST2P simulation (Fig. 14c) the latter flow is able to
560 penetrate all over the northern Adriatic and the Sirocco is progressively confined along the eastern
561 border of the basin. As shown by the vertical sections (d3, see Fig. 1b for the location) of potential
562 temperature and tangent wind component, drawn across the convergence area in the middle of the
563 Adriatic basin (Fig. 15), SST change has a critical impact on the PBL structure, which influence the
564 dynamical evolution and superposition between the two flows. Higher SST (SIR-03-SST2P) makes
565 the low-level Sirocco flow more buoyant, so that it is forced to rise over the dry southwesterly flow
566 from the Apennines and it is progressively displaced eastward together with the moisture advection
567 feeding the precipitation. Conversely, in SIR-03-SST2M (and to a lesser extent also in the SIR-03-
568 CNTRL), the southwesterly flow is not able to penetrate and to displace the Sirocco wind over the
569 Adriatic (Figs. 15a, b) and the low-level flow over the sea is not markedly modified. However, this
570 behaviour explains only the westward shift of the rainfall patterns in SIR-03-SST2P shown in Fig.
571 3e, f. To better explain the large sensitivity of the precipitation to different SST, vertical profiles are
572 computed to characterize the impinging flow over the Adriatic, upstream of the orography, by
573 taking an average of the meteorological fields over an area of about 20 x 20 km centred in 45.3 N,
574 13.0 E. Profiles (Fig. 16) are computed at 0900 UTC, 15 September 2006, two hours later than the
575 vertical sections. The vertical profile for SIR-03-SST2P shows a warmer and drier atmosphere in
576 the lower layers (up to 950 hPa) with southerly winds due to the air descending from the Apennines
577 and turning once over the Adriatic (as clearly shown also in Fig. 14). Conversely, SIR-03-CNTRL
578 and SIR-03-SST2M profiles indicate southeasterly (Sirocco) wind at the surface. However, both
579 SIR-03-SST2P and SIR-03-CNTRL profiles present high values of CAPE and are representative of
580 an environment prone to intense convective activity. Under these unstable conditions, even small
581 perturbations can trigger convection and produce large differences in precipitation, as actually
582 occurs in these two experiments. On the other hand, in SIR-03-SST2M the instability of the vertical
583 profile is largely reduced and the moist almost neutral stratification is not supportive of intense
584 convective precipitation.
585 Finally, for SIR-02 case, rainfall is not particularly sensitive to SST changes, although the dynamics
586 of the events is very similar to SIR-01 case. The vertical thermodynamic profiles simulated by
587 MOLOCH (not shown) indicate that the impact of SST is very limited on the PBL structure and not

sufficient to change the flow regime with respect to the orography. A flow over condition persists in all the simulations with only a minor effect on its intensity that determines small differences in the precipitation field. This result underlines the fact that when the SST does not determine a change of the PBL structure large enough to modify the flow regime, the effects on precipitation are almost negligible.

6.2 Bora cases.

The same procedure, aimed at identifying the dynamical processes that relate SST changes with precipitation patterns, is applied for the three Bora events, and the meteorological variables are analysed on vertical sections (see Figs. 6 and 8 for sections location).

As described in Section 4.1 for the simulation of BOR-01 event, the main effect of different SST initializations is to modify the low-level wind field (Fig. 6), displacing the line of convergence between Bora and the warmer cyclonic southeasterly wind. The different interaction between these two flows is responsible for different precipitation patterns. Figure 17 shows potential temperature and tangent wind component over a section drawn across the Adriatic along the southernmost Bora jet in correspondence with the area of convergence with southeasterly wind (Fig. 6). The contour lines mirror the Bora jet pattern (colder) and the southeasterly flow (warmer) that characterizes the low-level wind field from the surface up to 3000 m.

In BOR-01-CNTRL experiment (Fig. 17a), the Bora propagates over the eastern portion of the Adriatic basin, but towards the Italian coast it is progressively replaced by the warmer southeasterly flow. BOR-01-SST2M experiment (Fig. 17b) results in a colder and stably stratified PBL, which allows the low-level Bora flow to propagate over the Adriatic, against the competing southeasterly wind. The latter moist and warm flow is lifted over colder Bora layer as also confirmed by increased velocity of the wind at 850 hPa (not shown). Conversely, in BOR-01-SST2P a more mixed, warmer and less stable PBL is produced in correspondence to the low-level Bora flow, which is not able to confine the cyclonic southeasterly flow, and the latter can penetrate further to the north determining a displacement of the convergence line and thus of the associated precipitation. In both BOR-01-CNTRL and BOR-01-SST2M experiments, the selected section intercepts the area of sharp convergence close to the Italian coast, which determines intense and localized vertical velocities (clearly visible close to the western border of the sections). In BOR-01-SST2P, this uplift occurs to the north with respect to the selected section, due to the displacement of the convergence line.

Also in BOR-02 event, SST affects the low-level flow characteristics. As shown in Fig. 8, intensity and propagation of Bora over the Adriatic change among the experiments. In particular, as

described in Section 4.2, in BOR-02-SST2M the Bora jet located at around 43 N is deflected to its left in front of the Italian coast, while in BOR-02-SST2P the same Bora jet penetrates more inland. Vertical sections of cloud water/ice content and wind along this jet display the different behaviour of the northeasterly wind interacting with the Apennines (Fig. 18). In BOR-02-CNTRL simulation (Fig. 18a), except for a thin layer close to the surface, the flow is lifted over the orography where most of the condensation (and precipitation) occurs. In BOR-02-SST2M (Fig. 18b) the low-level flow is blocked, the main uplift occurs further upstream with respect to the Apennines and a lower amount of hydrometeors is produced. In BOR-02-SST2P (Fig. 18c) the flow over involves the entire impinging airflow, vertical velocity and condensation are much stronger and attain their maxima closer to the Apennines crest. Therefore, it is the stronger blocking effect of the Apennines, as the SST is decreased, that produces a weakening of the impinging wind even upstream of the orography. This is consistent with the fact that the effects of a mountain ridge having an average height of 1000-1500 m can extend more than 100 km upstream (Lin, 2007). The weakening of the winds reduces also the IWVF across the coast (presented in Section 5.2) that feeds the precipitation system.

Therefore, similarly to what was shown for BOR-01 case, it is the mesoscale circulation that provides most of the moisture feeding the precipitation, while SST does not affect markedly the water balance. Instead, SST plays an important role influencing the thermodynamic characteristics of the PBL and thus its interaction with the orography. The computation of the moist Froude number (Fr) confirms the above results. Fr is defined as the ratio between the wind speed impinging on the orography and the product of the significant orographic height and the static stability ($Fr=U/N\cdot h$). Fr (computed as in Davolio et al., 2016) is evaluated at 0600 UTC, 14 September 2012, assuming an average orographic height of 1000 m and vertical profiles of U and N representative of an area of about 20 x 20 km centred at 43.2 N, 14.7 E, thus sampling the impinging flow over the Adriatic Sea before being disturbed by the presence of the orography. Fr values are larger than one (1.35 for BOR-02-CNTRL, 1.40 for BOR-02-SST2P), in agreement with prevailing flow over conditions, even more evident with warmer SST. Fr decreases to 0.95 with colder SST, supporting the blocking effect of the orography.

Concerning the anticyclonic Bora events BOR-03, no relevant dynamical differences appear, since the change in SST by 2°C modifies only slightly the low-level wind intensity, which is stronger for BOR-03-SST2P. However, neither the stability nor the orographic regime of the low-level flow is changed and in all the three experiments Bora is forecast to flow over the Apennines where the direct orographic uplift is responsible for the precipitation. This is consistent with the large values of Fr that characterize the upstream low-level flow in all the simulations. The low-level moisture

content, largely ascribable to surface fluxes from the Adriatic Sea, which are relevant in this case, does not change significantly with different SST as to impact on the amount of precipitation over the Apennines.

It is worth mentioning that the majority of previous studies dealing with Bora were devoted to investigate the processes responsible for its generation along the eastern Adriatic. Some of these studies (Cesini et al., 2004; Kraljević and Grisogono, 2006; Grisogono and Belušić, 2009) showed that a warmer SST can modify the lee-side (with respect to the Dinaric Alps) flow stability, resulting in a more vigorous Bora over the Adriatic Sea. This is consistent with our results (see for example Fig. 8) since Bora is more intense in the SST2P simulations. We interpret the variation of Bora intensity in terms of a different interaction with the downstream orography (Apennines), since we focussed the attention mainly on the western Adriatic coast, where intense precipitation occurred. However, it can also be partially explained considering the effect of SST along the eastern Adriatic coast.

7. Conclusions

In the Adriatic basin, a semi enclosed sea surrounded by complex orography, strong low-level winds and intense air-sea exchanges are often harbinger of heavy precipitation events over Italy, since the Alpine and Apennines reliefs become exposed to intense impinging currents.

The present study, mainly based on diagnosing numerical simulations, aims at a better understanding of the role of the Adriatic SST on heavy precipitation associated with intense air-sea interaction. It tackles the problems from two different perspectives. From the one hand, it evaluates the impact of uncertainties in SST analysis, used to initialize NWP models, on severe weather predictions. On the other hand, it also investigates the physical processes through which the SST (uncertainty) possibly modifies location and intensity of heavy precipitation. The former is a relevant topic especially for operational forecasting activities; the latter allows to improve our knowledge on the mechanisms that often lead to severe weather in the Mediterranean area, in particular around the Adriatic basin, focusing the attention on those processes that modify the low-level flow characteristics and, consequently, its dynamics and eventually the interaction with the complex orography surrounding the basin. Only few preceding studies, if any, attempted to relate heavy precipitation over Italy and the Adriatic SST under intense Bora or Sirocco wind conditions. In fact, for Bora the main interest was placed on the study of the mechanisms associated with its generation and effects, including turbulence, near the eastern Adriatic coast (e.g. Grisogono and Belušić, 2009). For Sirocco, the attention was mainly focused on mesoscale dynamics, convection

690 and orographic effects (e.g. Barbi et al., 2012), but not on the possible contribution of the Adriatic
691 Sea, in terms of moisture and heat supply.
692 For this purpose, six different precipitation events, three associated with persistent moist
693 southeasterly flow (Sirocco), and three with strong and long-lasting cold northeasterly flow (Bora),
694 are selected and studied through high-resolution numerical simulations. A sensitivity analysis of
695 modelled precipitation to SST uncertainties is performed, increasing/decreasing the initial SST by
696 2°C over the Adriatic Sea.
697 For the above consideration and since we are interested in precipitation over Italy, it is
698 straightforward to focus the attention on processes associated with air-sea interaction, that
699 determine the amount of heat and moisture fluxes from the Adriatic Sea, and on low-level flow
700 thermodynamic characteristics, especially its stability and its interaction with the orography. Along
701 this line, after a dynamical analysis and the application of different diagnostic tools for the
702 evaluation of the integrated water vapour fluxes and for the atmospheric water budget computation,
703 some novel results have emerged from the present study, summarized as follows.
704 Numerical simulations reveal that the response of intense precipitation patterns to SST variations
705 (uncertainties) is complex since it involves non-linear effects associated with flow regimes in
706 response to the orographic forcing. Therefore, results modify the simplistic representation that
707 associates more intense precipitation with increasing SST, as a consequence of a larger degree of
708 moistening of the low-level flow during its passage over the sea. In fact, it is shown that in the
709 Adriatic basin the atmospheric water budget is not influenced markedly by the evaporation from the
710 sea, regardless of the SST initialization. It is instead modulated primarily by large-scale/mesoscale
711 circulation. The contribution to the water budget due to evaporation from the Adriatic Sea is
712 relevant only in the case of anticlyclonic Bora, when the low-level flow is particularly dry and there
713 is no cyclonic circulation providing moisture aloft. Nevertheless, also in that case, the impact of
714 SST uncertainties on precipitation is quite limited.
715 However, SST plays an important role on heavy precipitation associated with Bora and Sirocco, but
716 its effect is indirect and involves the modification of the PBL characteristics. Changes induced in
717 the thermodynamic profile and in the low-level stability can be critical in order to determine the
718 interaction between converging low-level flows or to establish the flow regime in response to
719 orographic forcing. As also supported by the orographic Froude number computation, if the flow
720 conditions are close to the transition between flow over and flow around (Lin, 2007), different SST
721 may alter the precipitation pattern favouring airflow rising over the mountain or flow retardation,
722 deviation and blocking upstream. For some cases, the SST uncertainty is not large enough to
723 modify the low-level dynamics, and its impact on heavy precipitation forecasts results almost

negligible. Conversely, if the atmospheric profile is particularly unstable, small perturbation as those associated with SST variations can trigger convective activity over the sea, changing the precipitation pattern almost randomly.

SST turns out to be important for precipitation prediction in case of both Bora and Sirocco, despite the different fetch, which is markedly larger for southeasterly flow, given the morphology of the basin. Therefore, the results point out that even for short-range forecasts, the precise definition of the initial SST field can be important as well as its correct evolution during the event simulation, since it may affect mesoscale flow characteristics, and in turn the interaction with orography. However, SST initialization is not the only source of forecast error and as stated by Cassola et al. (2016) the large scale forcing needs to be accurately predicted first.

Acknowledgements

This work was supported by the Italian flagship project RITMARE. This work is a contribution to the HyMeX international programme. The authors are grateful to Francesco Silvestro (CIMA Foundation) and Andrea Cicogna, Agostino Manzato and Arturo Pucillo (OSMER - ARPA FVG) for kindly providing precipitation data and maps, and for fruitful discussions. The authors would also like to thank Andrea Buzzi and Piero Malguzzi for useful discussions and modelling support.

References

Barbi, A., Monai, M., Racca, R., Rossa, A.M., 2012. Recurring features of extreme autumnal rainfall events on the Veneto coastal area, Nat. Hazard Earth Syst. Sci., 12, 2463–2477. doi:10.5194/nhess-12-2463-2012.

Benetazzo, A., Bergamasco, A., Bonaldo, D., Falcieri, F.M., Sclavo, M., Langone, L., Carniel, S., 2014. Response of the Adriatic Sea to an intense cold air outbreak: dense water dynamics and wave-induced transport. Progress in Oceanography 128, 115-138.

Berthou, S., Mailler, S., Drobinski, P., Arsouze, T., Bastin, S., Béranger, K. and Lebeaupin Brossier, C., 2014. Prior history of Mistral and Tramontane winds modulates heavy precipitation events in southern France. Tellus A 66, 24064, http://dx.doi.org/10.3402/tellusa.v66.24064.

Berthou, S., Mailler, S., Drobinski, P., Arsouze, T., Bastin, S., Béranger, K., Lebeaupin Brossier, C., 2015. Sensitivity of an intense rain event between an atmosphere-only and atmosphere ocean regional coupled model: 19 September 1996. Q. J. R. Meteorol. Soc. 141, 258–271. doi:10.1002/qj.2355.

Berthou, S., Mailler, S., Drobinski, P., Arsouze, T., Bastin, S., Béranger, K., Flaounas, E., Lebeaupin Brossier, C., Somot, S., Stéfanon, M., 2016. Influence of submonthly air-sea coupling on

heavy precipitation events in the Western Mediterranean basin. Q. J. R. Meteorol. Soc. 142, 453-471. doi:10.1002/qj.2717.

Billett, S.J., Toro E.F., 1997. A On WAF-Type Schemes for Multidimensional Hyperbolic Conservation Laws. Journal of Computational Physics 130,1 1-24.

Booth, J.F., Thompson, L., Patoux, J., Kelly, K.A., 2012. Sensitivity of midlatitude storm intensification to perturbations in the sea surface temperature near the Gulf Stream. Mon. Weather Rev. 140, 1241-1256. doi:10.1175/MWR-D-11-00195.1.

Borga, M., Boscolo, P., Zanon, F., Sangati, M., 2007. Hydrometeorological analysis of the 29 August 2003 flash flood in the Eastern Italian Alps. J. Hydrometeorol., 8, 1049–1067.

Buzzi, A., Tibaldi, S., 1978. Cyclogenesis in the lee of the Alps: A case study. Q. J. R. Meteorol. Soc. 104, 271–287. doi:10.1002/qj.49710444004.

Buzzi, A., D'Isidoro, M., Davolio, S., 2003. A case-study of an orographic cyclone south of the Alps during the MAP SOP. Q. J. R. Meteorol. Soc. 129, 1795–1818. doi:10.1256/qj.02.112.

Buzzi A., Davolio S., Malguzzi P., Drofa O., Mastrangelo D. 2014. Heavy rainfall episodes over Liguria of autumn 2011: Numerical forecasting experiments. Nat. Hazards Earth Syst. Sci. 14: 1325–1340.

Buzzi, A., Davolio, S., Malguzzi, P., Drofa, O., Mastrangelo, D., 2014. Heavy rainfall episodes over Liguria of autumn 2011: numerical forecasting experiments. Nat. Hazard Earth Syst. Sci. 14, 1325–1340.

Cassola, F., Ferrari F., Mazzino A., Miglietta M.M., 2016. The role of the sea on the flash floods events over Liguria (northwestern Italy). Geophys. Res. Lett. 43, 3534-3542.

Cesini, D., Morelli, S., Parmiggiani, F., 2004. Analysis of an intense Bora event in the Adriatic area. Nat. Hazards Earth Syst. Sci. 4, 323-337.

Davolio, S., Mastrangelo, D., Miglietta, M.M., Drofa, O., Buzzi, A., Malguzzi, P., 2009. High resolution simulations of a flash flood near Venice. Nat. Hazards Earth Syst. Sci. 9, 1671–1678. doi:10.5194/nhess-9-1671-2009.

Davolio, S., Stocchi, P., Carniel, S., Benetazzo, A., Bohm, E., Ravaioli, M., Riminucci, F., Li X., 2015. Exceptional Bora outbreak in winter 2012. Validation and analysis of high-resolution atmospheric model simulations in the northern Adriatic area. Dynam. Atmos. Oceans 71, 1–20. doi: 10.1016/j.dynatmoce.2015.05.002.

Davolio, S., Volonté, A., Manzato, A., Pucillo, A., Cicogna, A., Ferrario, M.E., 2016. Mechanisms producing different precipitation patterns over north-eastern Italy: insights from HyMeX-SOP1 and previous events. Q. J. R. Meteorol. Soc. 142, 188–205. doi:10.1002/qj.2731.

791 Davolio, S., Henin, R., Stocchi, P., Buzzi, A., 2017. Bora wind and heavy persistent precipitation:
792 atmospheric water balance and role of air-sea fluxes over the Adriatic Sea. Q. J. R. Meteorol. Soc.
793 143, 1165-1177. doi:10.1002/qj.3002.
794 De Zolt, S., Lionello, P., Malguzzi, P., Nuhu, A., Tomasin, A., 2006. The disastrous storm of 4
795 November 1966 on Italy. Nat. Hazards Earth Syst. Sci. 6, 861-879. doi:10.5194/nhess-6-861-2006.
796 Donlon, C.J., Martin, M., Stark, J., Roberts-Jones, J., Fiedler, E., Wimmer, W., 2012. The
797 Operational Sea Surface Temperature and Sea Ice Analysis (OSTIA) system, Remote Sens.
798 Environ. 116, 140–158. http://dx.doi.org/10.1016/j.rse.2010.10.017.
799 Dorman, C.E., Carniel, S., Cavaleri, L., Sclavo, M., Chiggiato, J., et al., 2007. February 2003
800 marine atmospheric conditions and the Bora over the northern Adriatic, J. Geophys. Res., 112,
801 C03S03. doi:10.1029/2005JC003134.
802 Drofa, O.V., Malguzzi, P., 2004. Parameterisation of microphysical processes in a non-hydrostatic
803 prediction model. Proc. 14th Intern. Conf. on Clouds and Precipitation (ICCP), 19–23 July 2004,
804 Bologna, Italy, 1297–1300.
805 Ducrocq, V., Braud, I., Davolio, S., Ferretti, R., Flamant, C., Jansa, A., Kalthoff, N., Richard, E.,
806 Taupier-Letage, I., Ayral, P.-A., Belamari, S., Berne, A., Borga, M., Boudevillain, B., Bock, O.,
807 Boichard, J.-L., Bouin, M.-N., Bousquet, O., Bouvier, C., Chiggiato, J., Cimini, D., Corsmeier, U.,
808 Coppola, L., Cocquerez, P., Defer, E., Delanoë, J., Di Girolamo, P., Doerenbecher, A., Drobinski,
809 P., Dufournet, Y., Fourrié, N., Gourley, J.J., Labatut, L., Lambert, D., Le Coz, J., Marzano, F.S.,
810 Molinié, G., Montani, A., Nord, G., Nuret, M., Ramage, K., Rison, W., Roussot, O., Said, F.,
811 Schwarzenboeck, A., Testor, P., Van Baelen, J., Vincendon, B., Aran, M., Tamayo, J., 2014.
812 HyMeX-SOP1: the field campaign dedicated to heavy precipitation and flash flooding in the
813 northwestern Mediterranean. Bull. Am. Meteorol. Soc. 95, 1083–1100.
814 Duffourg, F., Ducrocq, V., 2011. Origin of the moisture feeding the Heavy Precipitating Systems
815 over Southeastern France. Nat. Hazards Earth Syst. Sci. 11, 1163-1178.
816 Duffourg, F., Ducrocq, V., 2013. Assessment of the water supply to Mediterranean heavy
817 precipitation: a method based on finely designed water budgets. Atmos. Sci. Lett. 14, 133–138.
818 doi:10.1002/asl2.429.
819 Ferretti, R., Pichelli, E., Gentile, S., Maiello, I., Cimini, D., Davolio, S., Miglietta, M.M.,
820 Panegrossi, G., Baldini, L., Pasi, F., Marzano, F.S., Zinzi, A., Mariani, S., Casaioli, M., Bartolini,
821 G., Loglisci, N., Montani, A., Marsigli, C., Manzato, A., Pucillo, A., Ferrario, M.E., Colaiuda, V.,
822 Rotunno, R., 2014. Overview of the first HyMeX Special Observation Period over Italy:
823 Observations and model results. Hydrol. Earth Syst. Sci. 18, 1953–1977. doi:10.5194/hess-18-1953.

824 Göhm, A, Mayr, GJ. 2005. Numerical and observational case-study of a deep Adriatic Bora. Q. J.
825 R. Meteorol. Soc. 131, 1363–1392.
826 Grazzini, F., 2013. Cold spell prediction beyond a week: extreme snowfall events in February 2012
827 in Italy. ECMWF Newsl. 136, 31–35.
828 Grisogono, B., Belušić, D., 2009. A review of recent advances in understanding the meso- and
829 microscale properties of the severe Bora wind. Tellus A 61, 1–16. doi:10.1111/j.1600-
830 0870.2008.00369.x.
831 Henin, R., 2015. Dynamics of Bora wind over the Adriatic Sea: atmospheric water balance and role
832 of air-sea fluxes and orography. Master Thesis, http://amslaurea.unibo.it/8915 (accessed 09 May
833 2017).
834 Horvath, K., Ivatek-Sahdan, S., Ivančan-Picek, B., Grubišić, V., 2009. Evolution and structure of
835 two severe cyclonic Bora events: Contrast between the northern and southern Adriatic. Weather
836 Forecast. 24, 946-964.
837 Kain JS., 2004. The Kain–Fritsch convective parametrization: an update. J. Appl. Meteorol. 43,
838 170–181.
839 Katsafados, P., Mavromatidis, E., Papadopoulos, A., Pytharoulis, I., 2011. Numerical simulation of
840 a deep Mediterranean storm and its sensitivity on sea surface temperature. Nat. Hazards Earth Syst.
841 Sci. 11, 1233–1246. doi:10.5194/nhess-11-1233-2011.
842 Kraljević, L., Grisogono B., 2006. Sea-surface temperature effects on 3D Bora-like flow. Meteorol.
843 Zeit. 15, 169–177. doi: 10.1127/0941-2948/2006/0111.
844 Lebeaupin, C., Ducrocq, V. Giordani, H., 2006. Sensitivity of torrential rain events to the sea
845 surface temperature based on high-resolution numerical forecasts. J. Geophys. Res. 111, D12110.
846 doi:10.1029/2005JD006541.
847 Lin Y.L., 2007. Mesoscale Dynamics. Cambridge University Press: New York, NY.
848 Ludwig, P., Pinto, J.G., Reyers, M., Gray, S.L., 2014. The role of anomalous SST and surface
849 fluxes over the southeastern North Atlantic in the explosive development of windstorm Xynthia. Q.
850 J. R. Meteorol. Soc. 140, 1729-1741. doi:10.1002/qj.2253.
851 Maiello, I., Gentile, S., Ferretti, R., Baldini, L., Roberto, N., Picciotti, E., Alberoni, P.P., Marzano,
852 F.S., 2016. Effects of multiple doppler radar data assimilation on the □numerical□simulation of a
853 flash flood event during the HyMeX □campaign.Hydrol. Earth Syst. Sci. Discuss.,
854 doi:10.5194/hess-2016-320.
855 Malguzzi, P., Grossi, G., Buzzi, A., Ranzi, R., Buizza, R., 2006. The 1966 “century” flood in Italy:
856 A meteorological and hydrological revisitation. J. Geophys. Res. 111, D24106,
857 doi:10.1029/2006JD007111.

858 Manzato, A., 2007. The 6 h climatology of thunderstorms and rainfalls in the Friuli Venezia Giulia
859 plain. Atmos. Res. 83, 336-348.
860 Manzato, A., Davolio, S., Miglietta, M.M., Pucillo, A., Setvak, M., 2015. 12 September 2012: A
861 supercell outbreak in NE Italy? Atmos. Res. 153, 98–118.
862 Meredith, E.P., Semenov, V.A., Maraun, D., Park, W., Chernokulsky, A.V., 2015: Crucial role of
863 Black Sea warming in amplifying the 2012 Krymsk precipitation extreme. Nature Geosc. 8, 615-
864 619. doi:10.1038/ngeo2483.
865 Mihanović, H., Vilibić, I., Carniel, S., Tudor, M., Russo, A., Bergamasco, A., Bubić, N.,
866 Ljubešić, Z., Viličić, D., Boldrin, A., Malačič, V., Celio, M., Comici, C., Raicich, F., 2013.
867 Exceptional dense water formation on the Adriatic shelf in the winter of 2012. Ocean Sci. 9, 561-
868 572. doi:10.5194/os-9-561-2013.
869 Miglietta, M.M., Moscatello, A., Conte, D., Mannarini, G., Lacorata, G, Rotunno, R., 2011.
870 Numerical analysis of a Mediterranean “hurricane” over south-eastern Italy: Sensitivity experiments
871 to sea surface temperature. Atmos. Res. 101, 412–426.
872 Morcrette J.J., Barker, H.W., Cole, J.N.S., Iacono, M.J., Pincus, R., 2008. Impact of a new radiation
873 package, McRad, in the ECMWF Integrated Forecasting System. Mon. Weather Rev. 136, 4773–
874 4798. http://dx.doi.org/10.1175/2008MWR2363.1.
875 Pastor, F., Estrela, M.J., Peñarrocha, D., Millan, M., 2001. Torrential rains on the Spanish coast:
876 modeling the effects of the sea surface temperature. J. Appl. Meteorol. 40, 1180-1195.
877 Pastor, F., Valiente, J.A., Estrela, M.J., 2015. Sea surface temperature and torrential rains in the
878 Valencia region: modelling the role of recharge areas. Nat. Hazards Earth Syst. Sci. 15, 1677–1693.
879 doi:10.5194/nhess-15-1677-2015.
880 Pullen, J., Doyle, J.D., Signell, R.P., 2006. Two-way air–sea coupling: a study of the Adriatic. Mon.
881 Weather Rev. 134, 1465–1483.
882 Pullen, J., Doyle, J.D., Haack, T., Dorman, C.D., Signell, R.P., Lee, C.M., 2007. Bora event
883 variability and the role of air-sea feedback. J. Geophys. Res. 112, C03S18.
884 doi:10.1029/2006JC003726.
885 Raicich, F., Malačič V., Celio, M., Giaiotti, D., Colucci, R.R., Cermelj, B., Pucillo, A., 2013.
886 Extreme air–sea interactions in the Gulf of Trieste (North Adriatic) during the strong Bora event in
887 winter 2012. J. Geophys. Res. (Oceans) 18, 5238–5250. doi:http://dx.doi.org/10.1002/jgrc.20398.
888 Rainaud, R., Lebeaupin Brossier, C., Ducrocq, V., Giordani, H., Nuret, M., Fourrié, N., Bouin, M.-
889 N., Taupier-Letage, I., Legain, D., 2016. Characterization of air–sea exchanges over the Western
890 Mediterranean Sea during HyMeX SOP1 using the AROME–WMED model. Q. J. R. Meteorol.
891 Soc. 142, 173–187. doi:10.1002/qj.2480.

892 Ricchi, A., Miglietta M.M., Falco, P.P., Benetazzo, A., Bonaldo, D., Bergamasco, A., Sclavo, M.,
893 Carniel S., 2016. On the use of coupled ocean-atmosphere-wave model during an extreme cold air
894 outbreak over the Adriatic Sea. Atmos. Res. 172–173, 48–65.
895 Ritter B., Geleyn JF., 1992. A comprehensive radiation scheme for numerical weather prediction
896 models with potential applications in climate simulations. Mon. Weather Rev. 120, 303–325.
897 Romaniello, V., Oddo, P., Tonani, M., Torrisi, L., Grandi, A., Pinardi, N., 2015. Impact of Sea
898 Surface Temperature on COSMO Forecasts of a Medicane over the Western Mediterranean Sea. J.
899 Earth Sci. and Engineering 5, 338-348.
900 Roxy, M., Tanimoto, Y., Preethi, B., Terray, P., Krishnan, R., 2013. Intraseasonal SST-precipitation
901 relationship and its spatial variability over the tropical summer monsoon region, Clim. Dyn. 41, 45.
902 doi:10.1007/s00382-012-1547-1.
903 Senatore, A., Mendicino, G., Knoche, H., Kunstmann, H., 2014. Sensitivity of modeled
904 precipitation to sea surface temperature in regions with complex topography and coastlines: A case
905 study for the Mediterranean. J. Hydrometeorol. 15, 2370-2396.
906 Smith R.B., 1979. The influence of mountains on the atmosphere. Adv. Geophys. 21, 87–230.
907 Stocchi, P., Davolio, S., 2016. Intense air-sea exchange and heavy rainfall: impact of the northern
908 Adriatic SST, Adv. Sci. Res. 1, 1–6.
909 Toy, M.D., Johnson, R.H., 2014. The influence of an SST front on a heavy rainfall event over
910 coastal Taiwan during TiMREX. J. Atmos. Sci. 71, 3223–3249.
911 Trenberth, K.E., Shea, D.J., 2005. Relationships between precipitation and surface temperature.
912 Geophys. Res. Lett. 32, 1–4. doi:10.1029/2005GL022760.
913 Tudor M., Ivatek-Sahdan S., Stanesic A., 2015. Assessment of sea surface temperatures provided in
914 the coupling files from ARPEGE and IFS. doi: 10.13140/RG.2.1.4431.8160,
915 https://www.researchgate.net/profile/Martina_Tudor/publication/283894579_Assessment_of_sea_s
916 urface_temperatures_provided_in_the_coupling_files_from_ARPEGE_and_IFS/links/5649a2d308a
917 e9f9c13ec1750.pdf (accessed 08 Feb. 2017).
918 Zampieri, M., Malguzzi, P., Buzzi, A., 2005. Sensitivity of quantitative precipitation forecasts to
919 boundary layer parameterization: A flash flood case study in the western Mediterranean. Nat.
920 Hazards Earth Syst. Sci. 5, 603–612. doi:10.5194/nhess-5-603-2005.
921

Table captions

Table 1: Selected Sirocco and Bora events. Initial conditions for BOLAM simulations (MOLOCH is initialized 3 hours later) are reported, together with the indication of the period of intense precipitation and of the type of event. The last column shows the maximum contribution to the atmospheric water budget provided by the surface latent heat fluxes from Adriatic Sea (see Sect. 5.2.2).

Figure captions

Figure 1: SIR-01 event: (a) ECMWF analysis at 0000 UTC, 11 Nov. 2012 of mean sea level pressure (black contour lines), 500 hPa geopotential height (colour shading); (b) 10-m wind at 0600 UTC, 11 Nov. 2012 (MOLOCH-CNTR, +15h forecast) and model orography (contour interval 500 m). The area shown in (a) represents the BOLAM integration domain, while in (b) the MOLOCH integration domain used for Sirocco events (SIR) simulations is shown. The three red lines in (b) indicate the location of the cross sections (d1, d2 and d3) shown in Figs. 12, 13 and 15; the black dashed rectangle identifies the box used for the water balance computation.

Figure 2: 24-h observed accumulated precipitation (mm) for the three Sirocco events: (a) SIR-01, 11 Nov. 2012, (b) SIR-02, 31 Oct. 2010 and (**c**) SIR-03, 15 Sep. 2006. Data provided by ARPAV and OSMER – ARPA FVG; courtesy of Andrea Cicogna.

Figure 3: Difference of 24-h accumulated precipitation (mm) fields between CNTRL and SST2M (a, c, e) or CNTRL and SST2P (b, d, f). SIR-01 case (a), (b), 11 Nov. 2012; SIR-02 case (c), (d), 31 Oct. 2010; SIR-03 case (e), (f), 15 September 2006. Red colour indicates areas where the CNTRL run is more rainy.

Figure 4: ECMWF analysis interpolated on the BOLAM grid (a) at 0000 UTC, 14 Sep. 2012 (BOR-02) and (b) at 0000 UTC, 31 Dec. 2014 (BOR-03). Mean sea level pressure (black contour lines), 500 hPa geopotential height (colour shading). The black rectangle in (a) indicates the MOLOCH integration domain used for Bora event (BOR) simulations.

Figure 5: 24-h accumulated precipitation (mm). MOLOCH CNTRL experiment for Bora events: (a) BOR-01 (10 Feb. 2012), (b) BOR-02 (14 Sep. 2012), and (c) BOR-03 (31 Dec. 2014).

Figure 6: 950 hPa equivalent potential temperature and wind for BOR-01 event. 24-h MOLOCH forecasts valid at 1500 UTC, 10 Feb. 2012, for experiment (a) BOR-01-CNTRL, (b) BOR-01-SST2M and (c) BOR-01-SST2P. Only wind exceeding 10 m s^{-1} is shown. The black line in (a) indicates the location of the cross section shown in Fig. 17.

Figure 7: Difference of 24-h accumulated precipitation (mm) fields between CNTRL and SST2M (a, c, e) or CNTRL and SST2P (b, d, f). BOR-01 event (a), (b), 10 Feb. 2012; BOR-02 event (c), (d), 14 Sep. 2012; BOR-03 event (e), (f), 31 Dec. 2014. Note that the label bar is different in (c) and (d). Red colour indicates areas where the CNTRL run is more rainy.

Figure 8: 10-m wind at 1000 UTC, 14 Sep. 2012. 19h MOLOCH forecasts for experiment (a) BOR-02-CNTRL, (b) BOR-02-SST2M and (c) BOR-02-SST2P. The black line in (a) indicates the location of the cross section shown in Fig. 18. The dashed rectangle in (c) indicates the box used for the water balance computation for all Bora cases.

Figure 9: Atmospheric water balance for the CNTRL experiments of Sirocco events: (a) SIR-01, (b) SIRO-02 and (c) SIRO-03. Individual contributions through each lateral sides (North, South, East, West) and from the bottom interface (surface latent heat fluxes and precipitation) are plotted.

Figure 10: Vertically integrated horizontal Water Vapour Flux (IWVF) along the Italian Adriatic coast (shown in the left part of the panel) computed for the three Bora events: at 1500 UTC, 10 Feb. 2012, BOR-01 (left); at 0900 UTC, 14 Sep. 2012, BOR-02 (middle); 0700 UTC, 31 Dec. 2014, BOR-03 (right) from MOLOCH simulations: CNTRL (black stars), SST2M (blue line), SST2P (red line). Note that for September event (central panel) the x-axis scale is different.

Figure 11: As in Fig. 9, but for the three Bora events: (a) BORA-01-CNTRL, (b) BORA-02-CNTRL, and (c) BORA-03-CNTRL. Note that in (b) the y-axis scale is different.

Figure 12: Cross sections (d1, location in Fig. 1b) of potential temperature (colour shading, K) and wind component tangent to the section, at 0900 UTC, 11 Nov. 2012 for (a) SIR-01-CNTRL, (b) SIR-01-SST2M and (c) SIR-01-SST2P MOLOCH experiments.

Figure 13: Cross sections (d2, location in Fig. 1b) of cloud water/ice content (colour shading, g kg^{-1}) and vertical wind velocity (m s^{-1}) (contour, starting from 1 m s^{-1}), at 0900 UTC, 11 Nov. 2012 for (a) SIR-01-CNTRL, (b) SIR-01-SST2M and (c) SIR-01-SST2P MOLOCH simulations.

Figure 14: Relative humidity (%) and 10-m wind at 1200 UTC, 15 Sep. 2006. MOLOCH simulations (a) SIR-03-CNTRL, (b) SIR-03-SST2M and (c) SIR-03-SST2P.

Figure 15: Cross sections (d3, location in Fig. 1b) of potential temperature (colour shading, K) and wind component tangent to the section, at 0700 UTC, 15 Sep. 2006 for (a) SIR-03-CNTRL , (b) SIR-03-SST2M and (c) SIR-03-SST2P MOLOCH experiments.

Figure 16: Skew T/log P thermodynamic diagrams at 0900 UTC, 15 Sep. 2006 (bold line indicates temperature, dotted line indicates dew point temperature, red dashed line indicates the saturation adiabatic curve from the lifting condensation level), computed from MOLOCH simulations: (a) SIR-03-CNTRL, (b) SIR-03-SST2M and (c) SIR-03-SST2P. The profiles are representative of an area of about 20 km x 20 km centred over the Adriatic Sea in 45.3 N, 13 E.

Figure 17: Cross sections of potential temperature (colour shading) and wind component tangent to the section, at 1500 UTC, 10 Feb. 2012 for (a) BOR-01-CNTRL, (b) BOR-01-SST2M and (c) BOR-01-SST2P MOLOCH experiments. Location of sections is shown in Fig. 6a.

Figure 18: Cross section (location in Fig. 8a) of cloud water/ice content (colour shading) and wind velocity tangent to the section (m s^{-1}), at 0900 UTC, 14 Sep. 2012 for (a) BOR-02-CNTRL, (b) BOR-02-SST2M and (c) BOR-02-SST2P MOLOCH experiments.

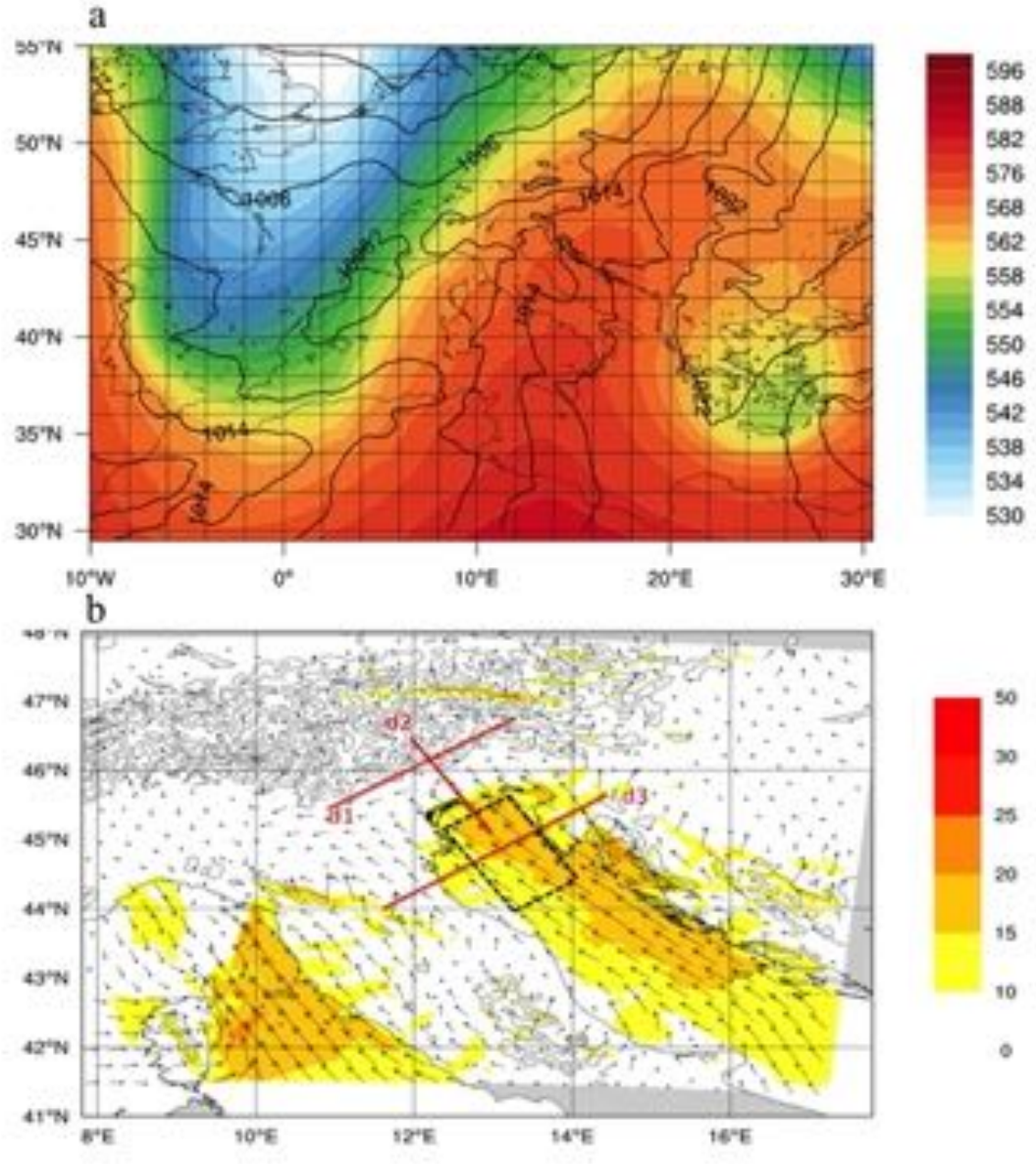
a
55°N
50°N
45°N
40°N
35°N
30°N
10°W
0°
10°E
20°E
30°E
1006
1010
1014
596
588
582
576
568
562
558
554
550
546
542
538
534
530
b
47°N
46°N
45°N
44°N
43°N
42°N
41°N
8°E
10°E
12°E
14°E
16°E
d1
d2
d3
50
30
25
20
15
10
0

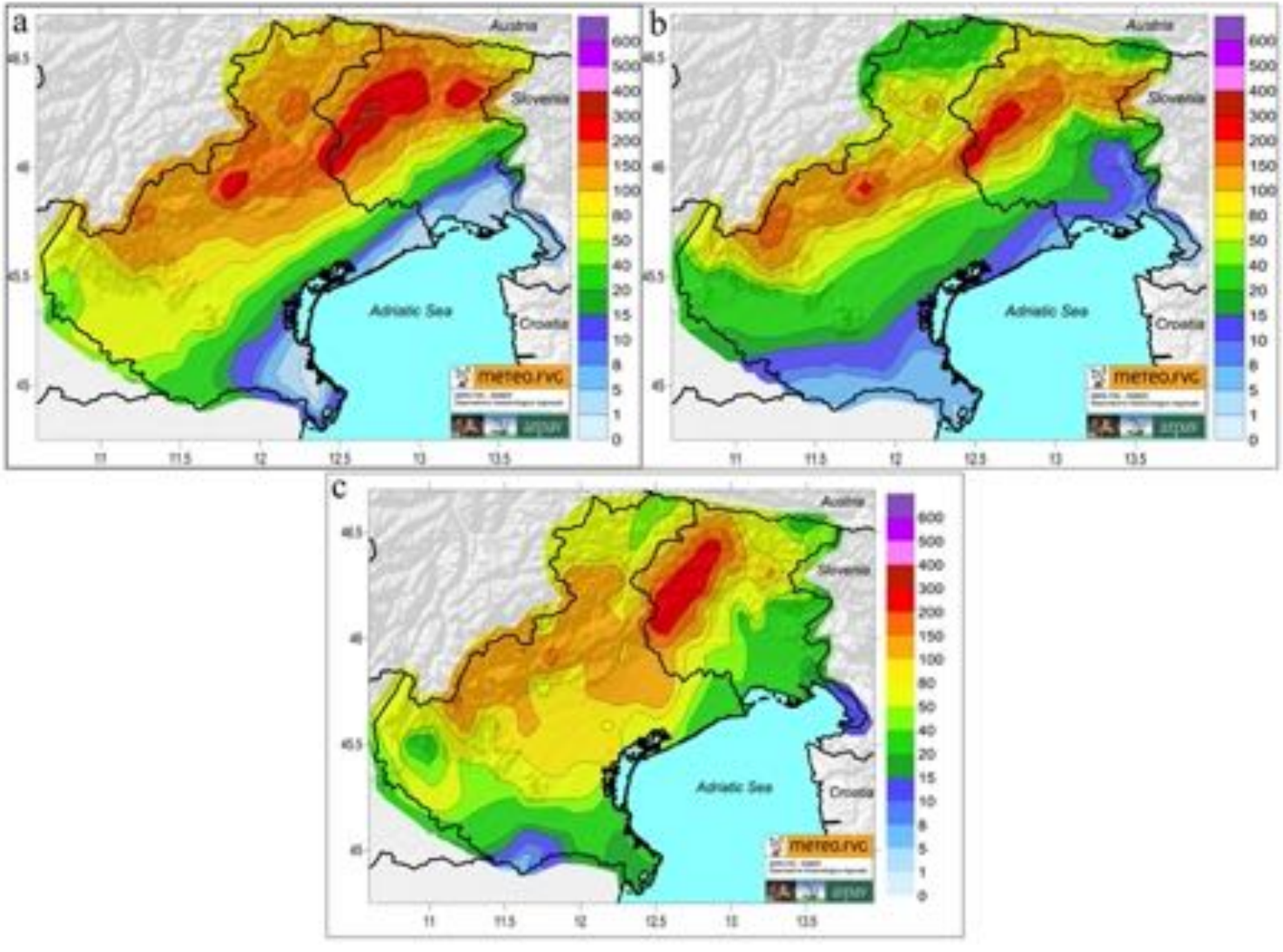
a
b
c
Austria
Slovenia
Adriatic Sea
Croatia
meteo.fvg
arpa
600
500
400
300
200
150
100
80
50
40
20
15
10
8
5
1
0
46.5
46
45.5
45
11
11.5
12
12.5
13
13.5

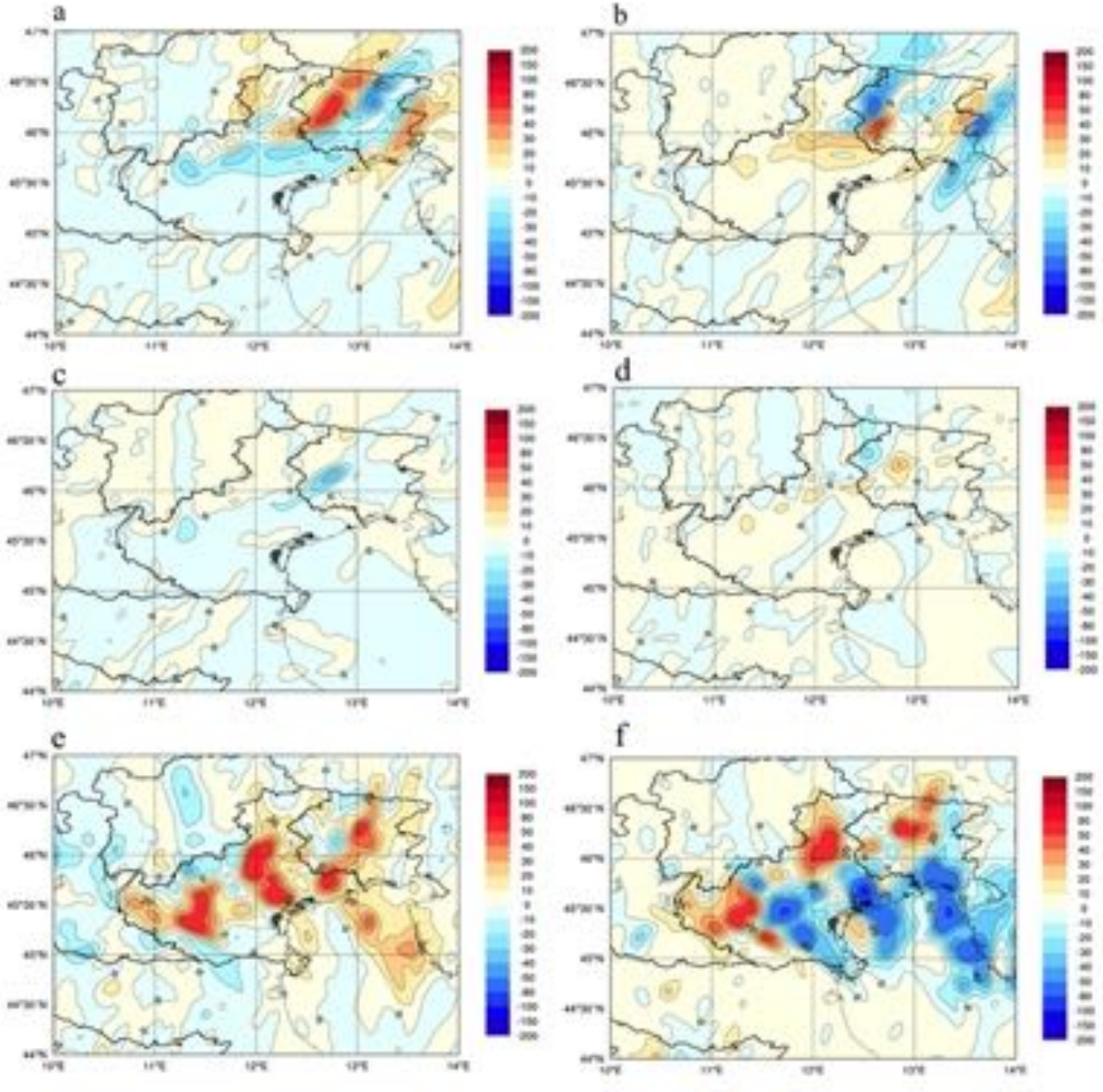
a
b
c
d
e
f

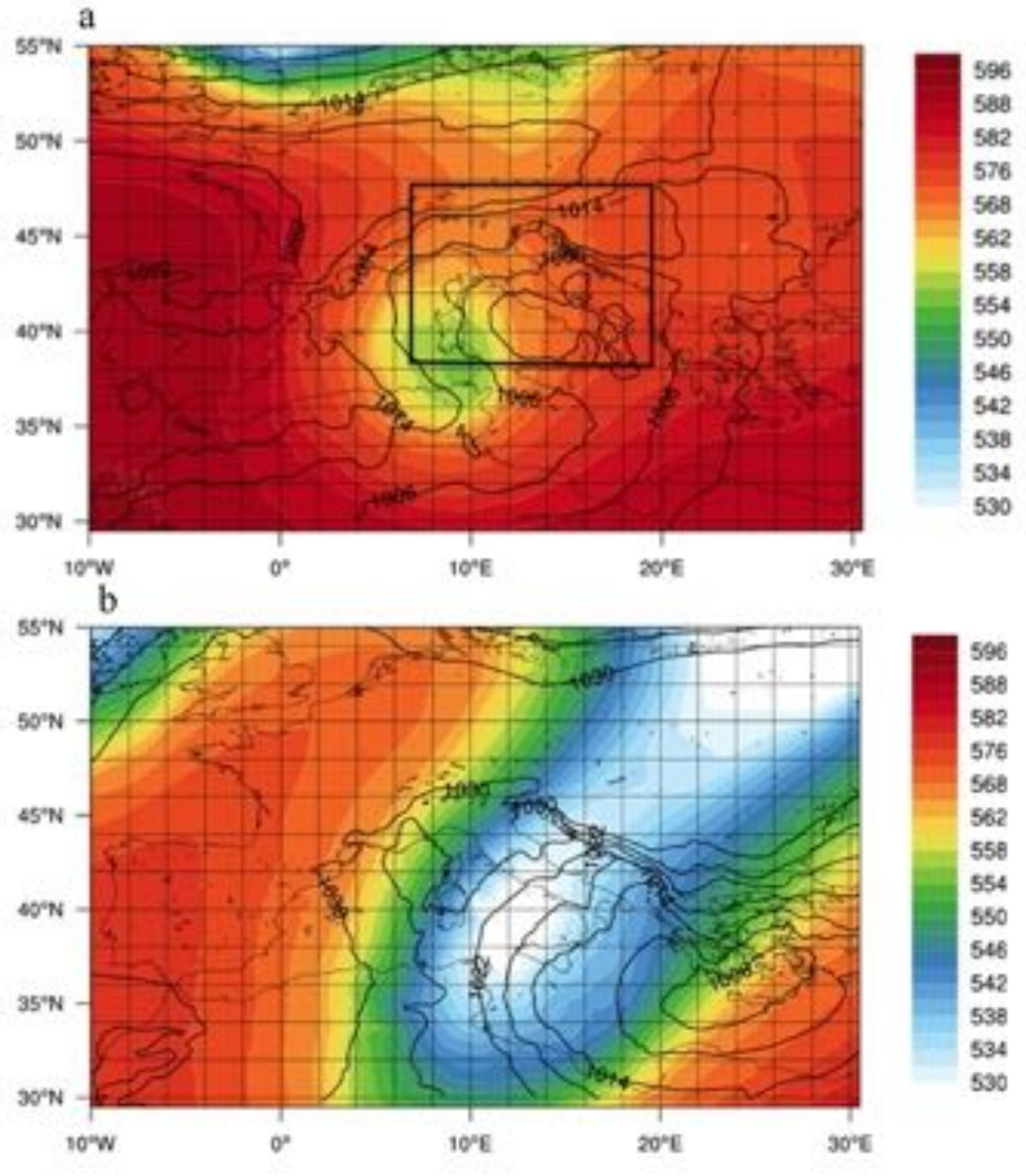
a
55°N
50°N
45°N
40°N
35°N
30°N
10°W
0°
10°E
20°E
30°E
596
588
582
576
568
562
558
554
550
546
542
538
534
530
b
55°N
50°N
45°N
40°N
35°N
30°N
10°W
0°
10°E
20°E
30°E
596
588
582
576
568
562
558
554
550
546
542
538
534
530

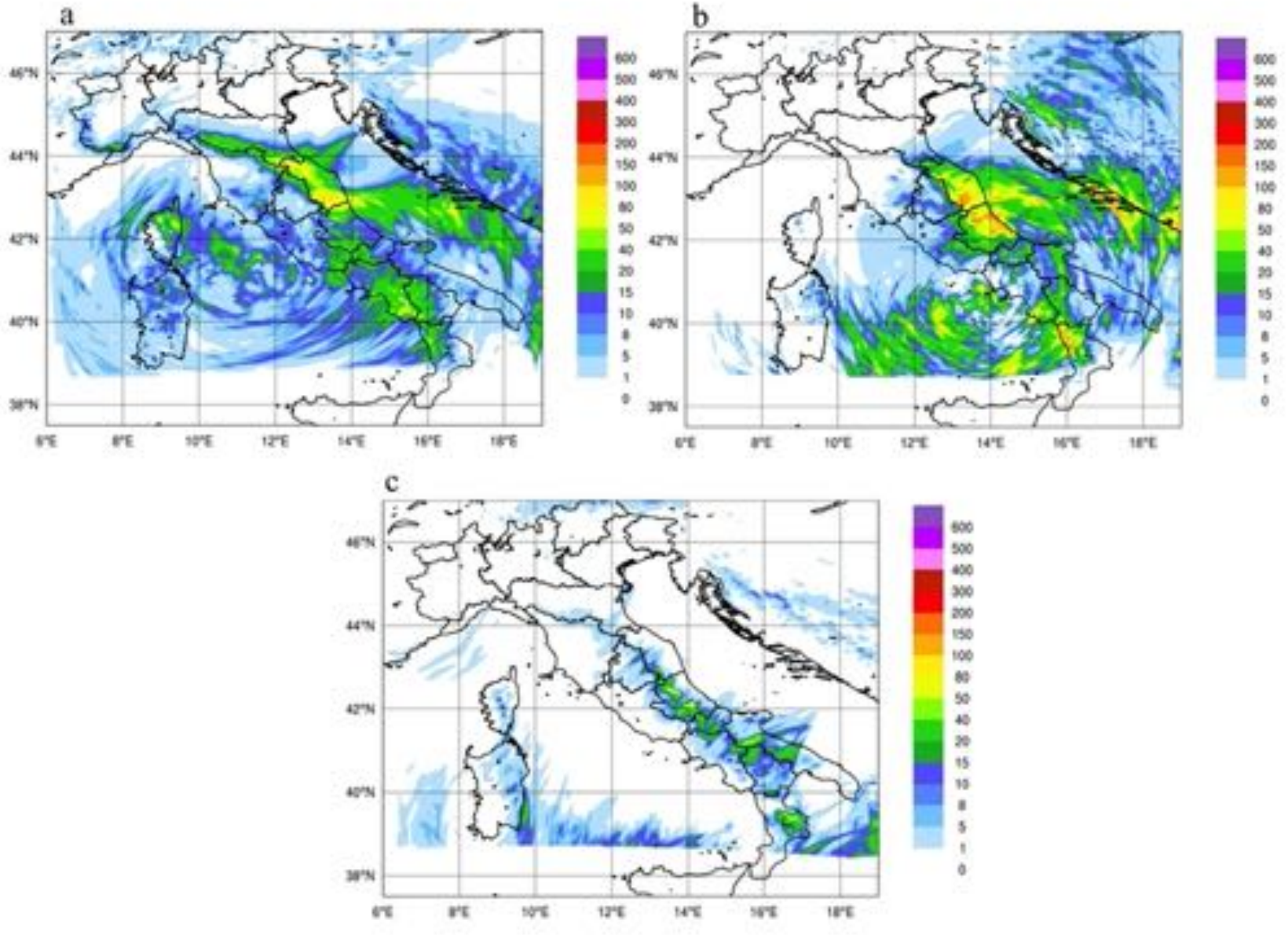
a
b
c
46°N
44°N
42°N
40°N
38°N
6°E
8°E
10°E
12°E
14°E
16°E
18°E
600
500
400
300
200
150
100
80
50
40
20
15
10
8
5
1
0

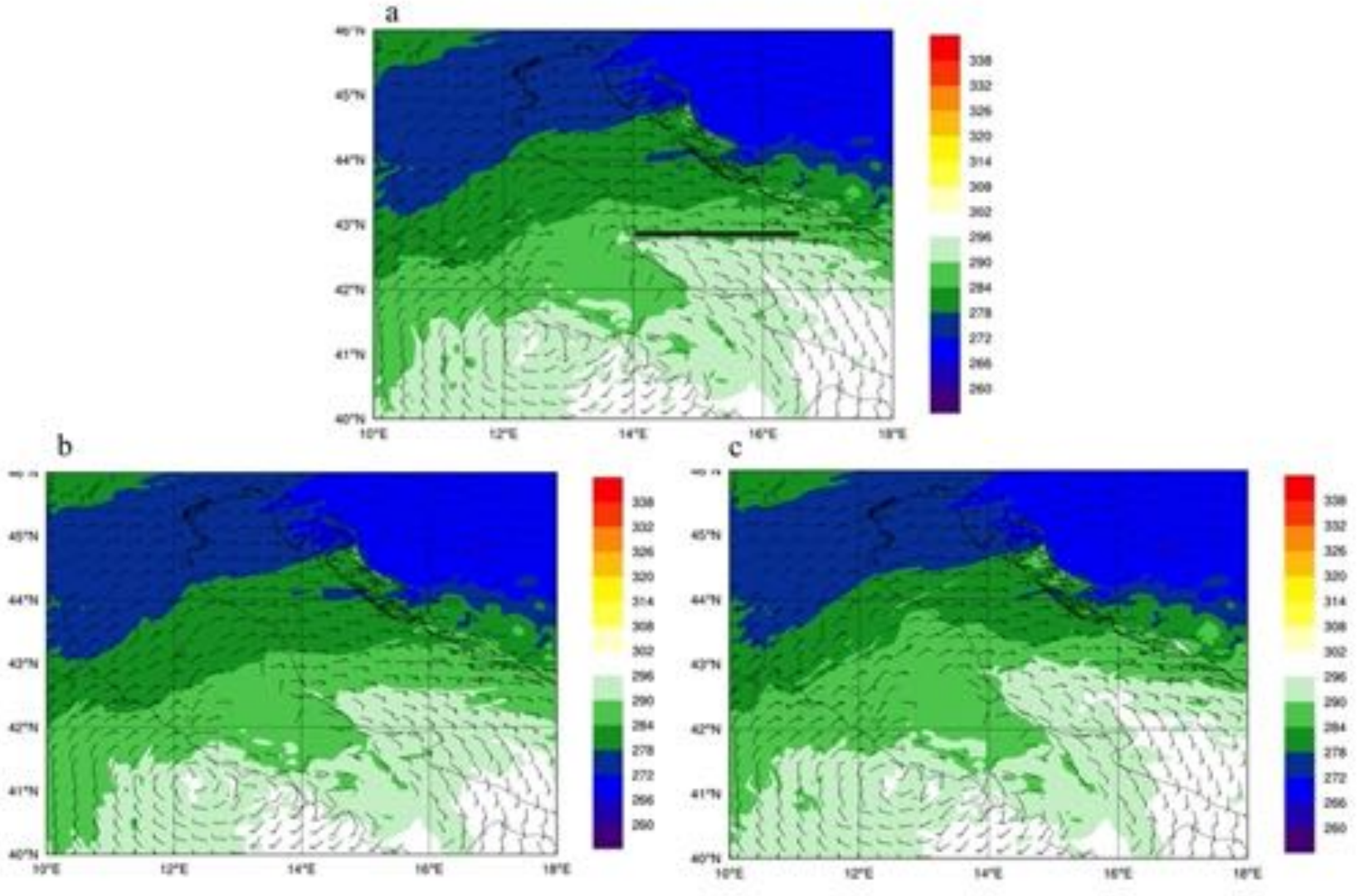
a
b
c
45°N
44°N
43°N
42°N
41°N
40°N
10°E
12°E
14°E
16°E
18°E
338
332
326
320
314
308
302
296
290
284
278
272
266
260

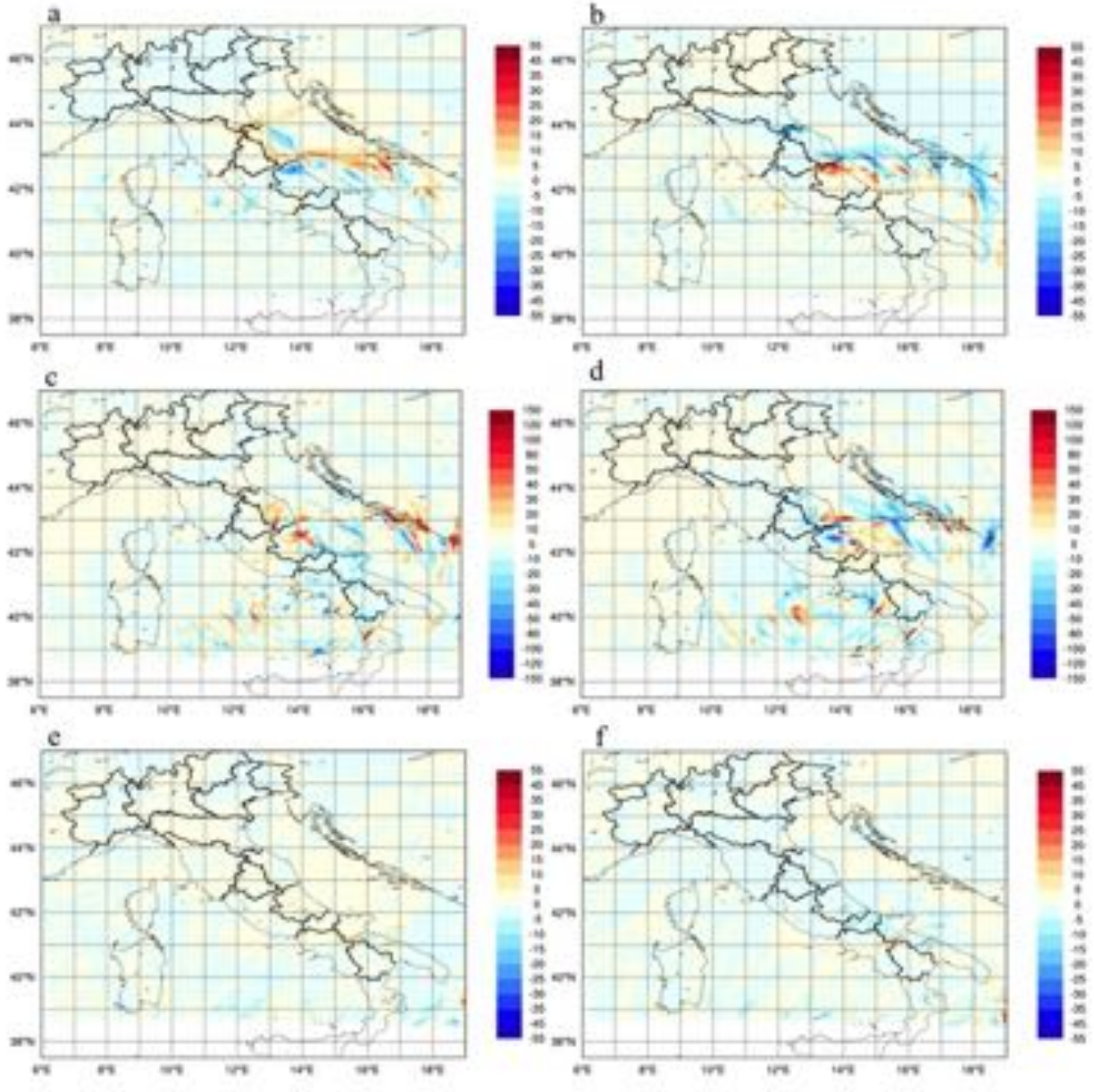
a
b
c
d
e
f

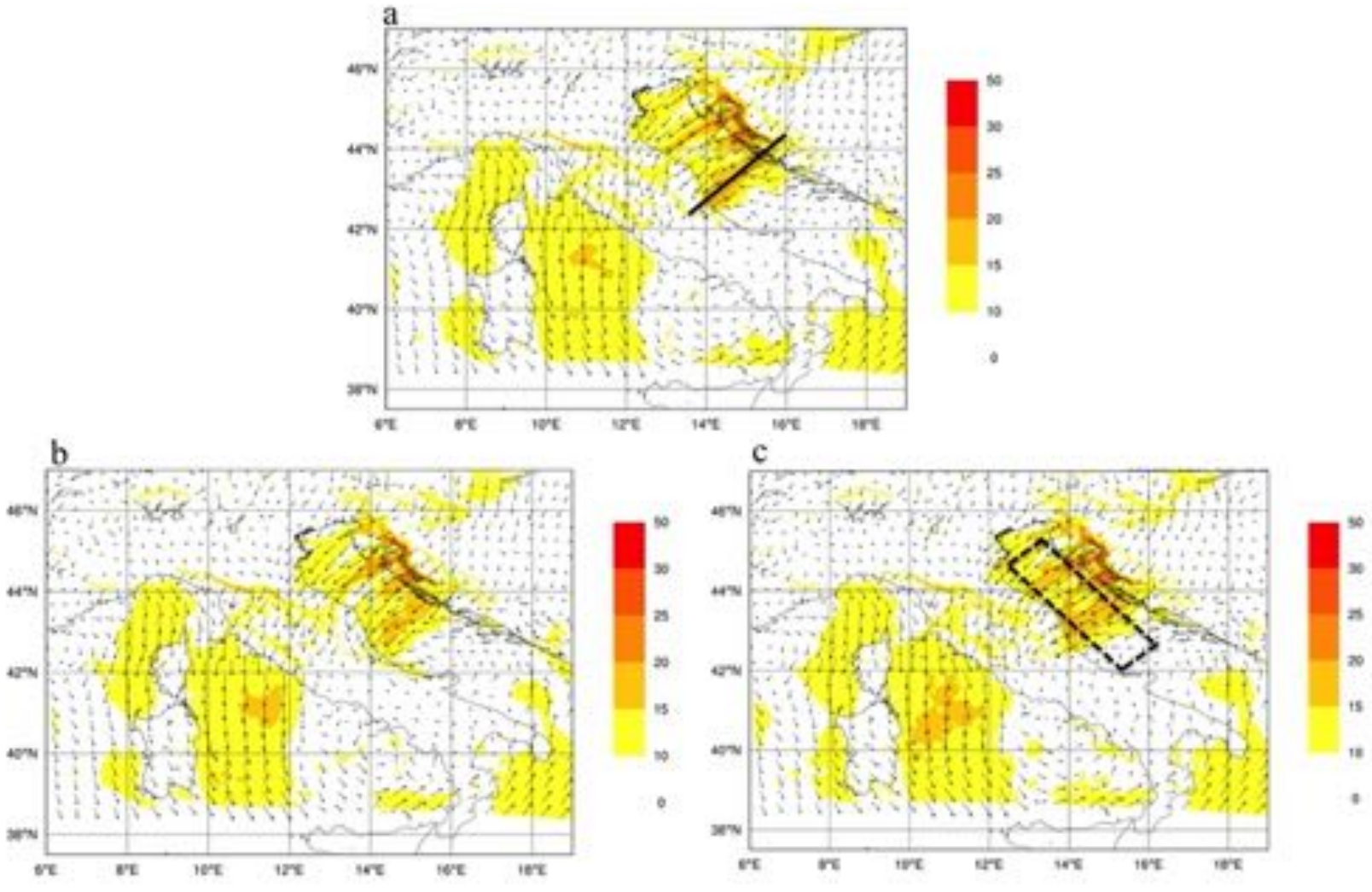
a
b
c
46°N
44°N
42°N
40°N
38°N
6°E
8°E
10°E
12°E
14°E
16°E
18°E
50
30
25
20
15
10
0

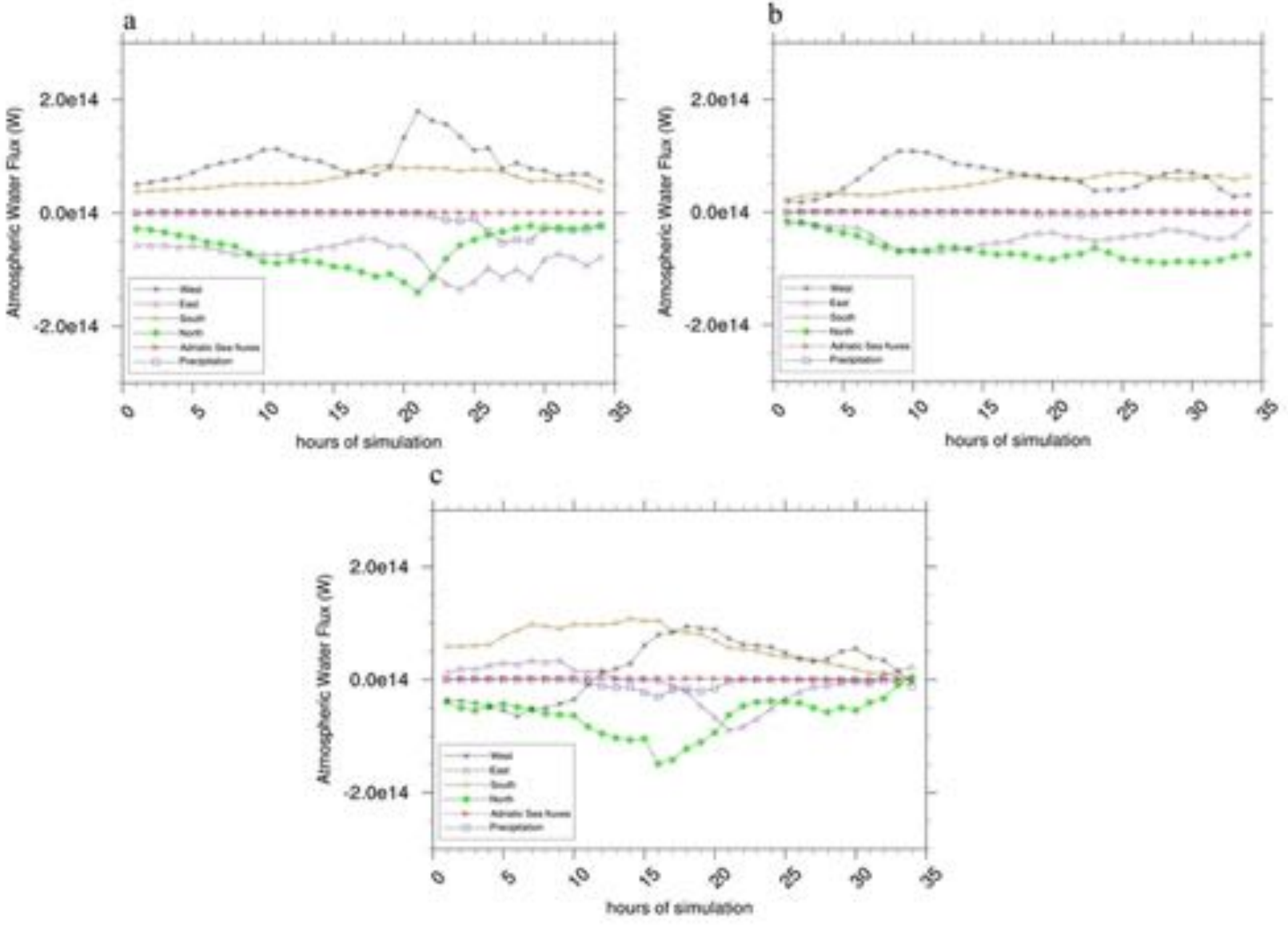
a
b
c
Atmospheric Water Flux (W)
2.0e14
0.0e14
-2.0e14
0
5
10
15
20
25
30
35
hours of simulation
West
East
South
North
Adriatic Sea fluxes
Precipitation

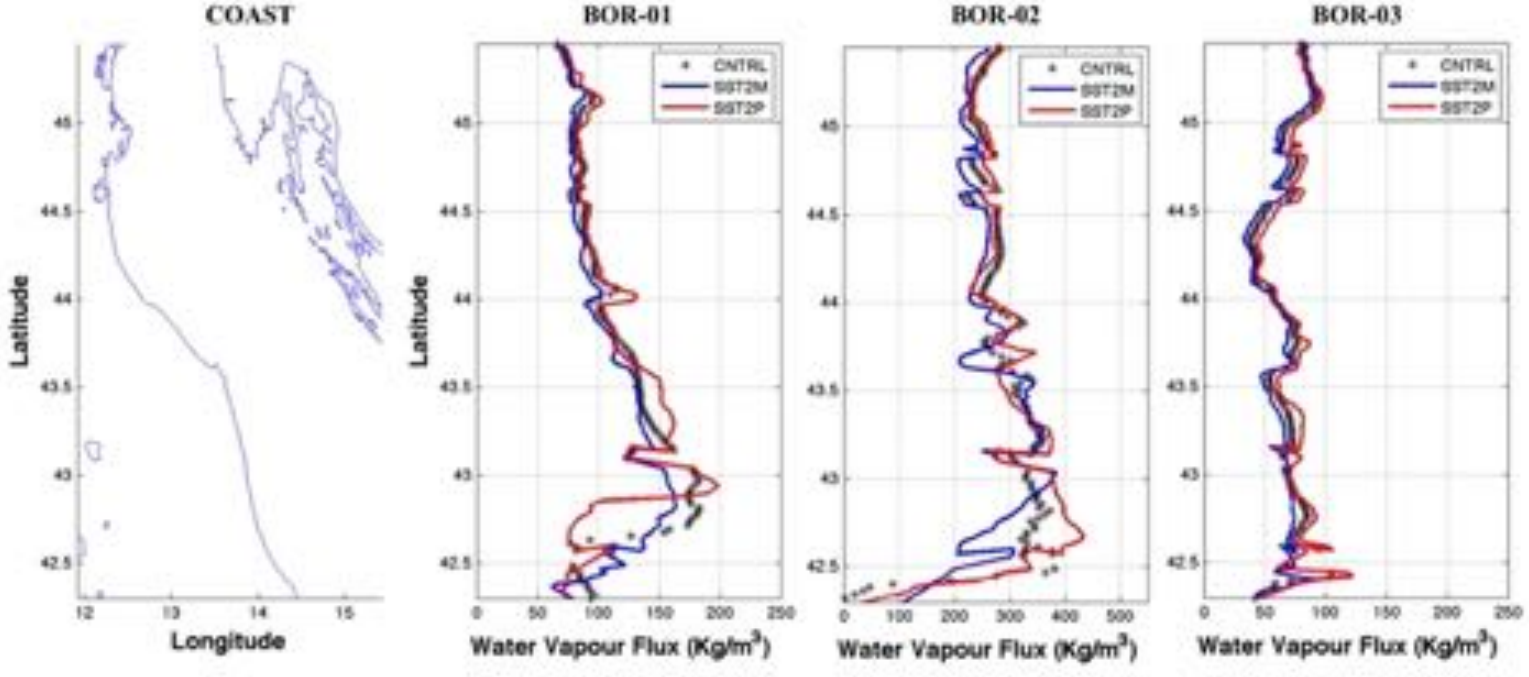
COAST
BOR-01
BOR-02
BOR-03
Latitude
Longitude
Water Vapour Flux (Kg/m3)
CNTRL
SST2M
SST2P

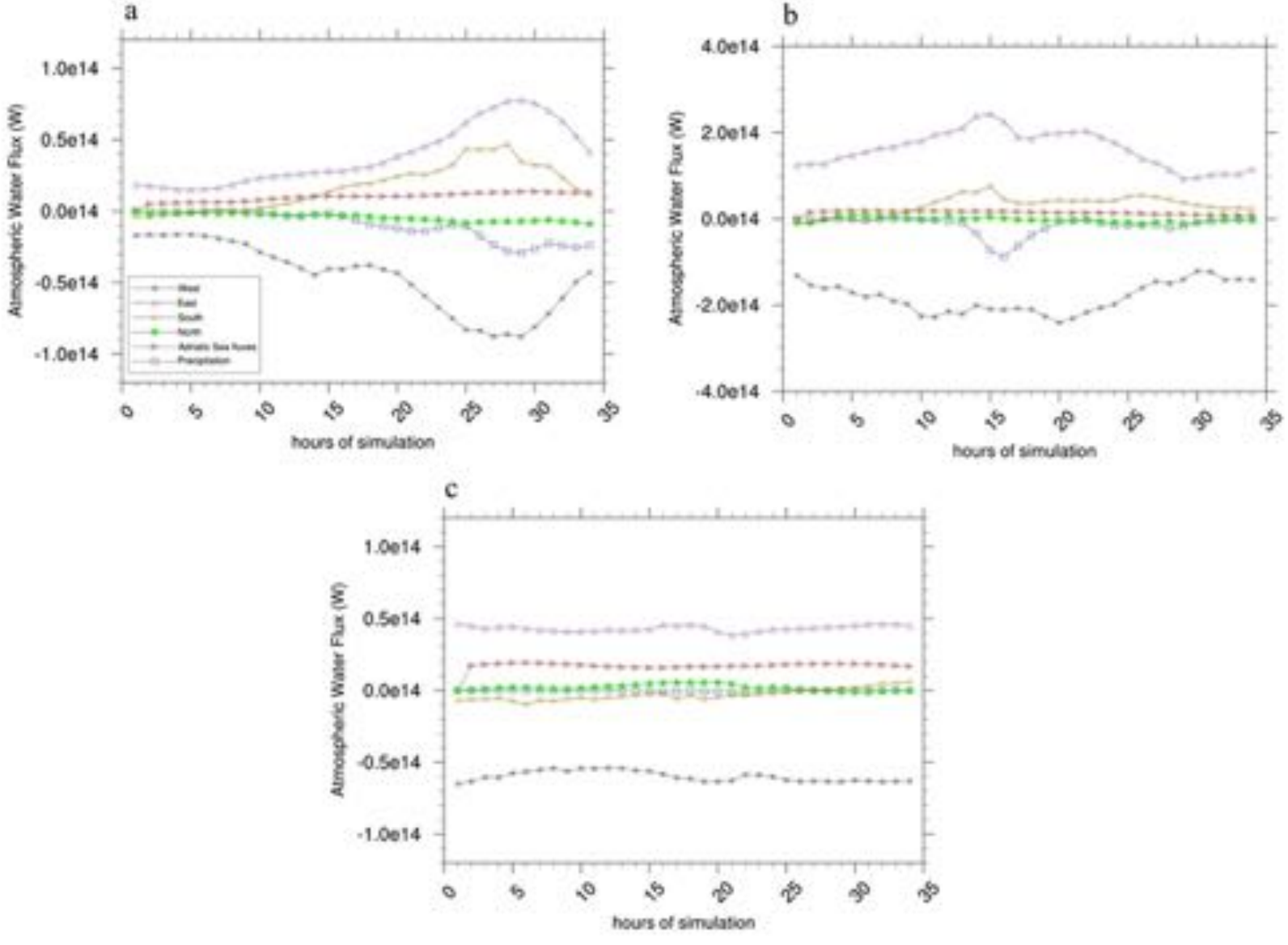
a
b
c
Atmospheric Water Flux (W)
hours of simulation
1.0e14
0.5e14
0.0e14
-0.5e14
-1.0e14
4.0e14
2.0e14
-2.0e14
-4.0e14
0
5
10
15
20
25
30
35
West
East
South
North
Adriatic Sea fluxes
Precipitation

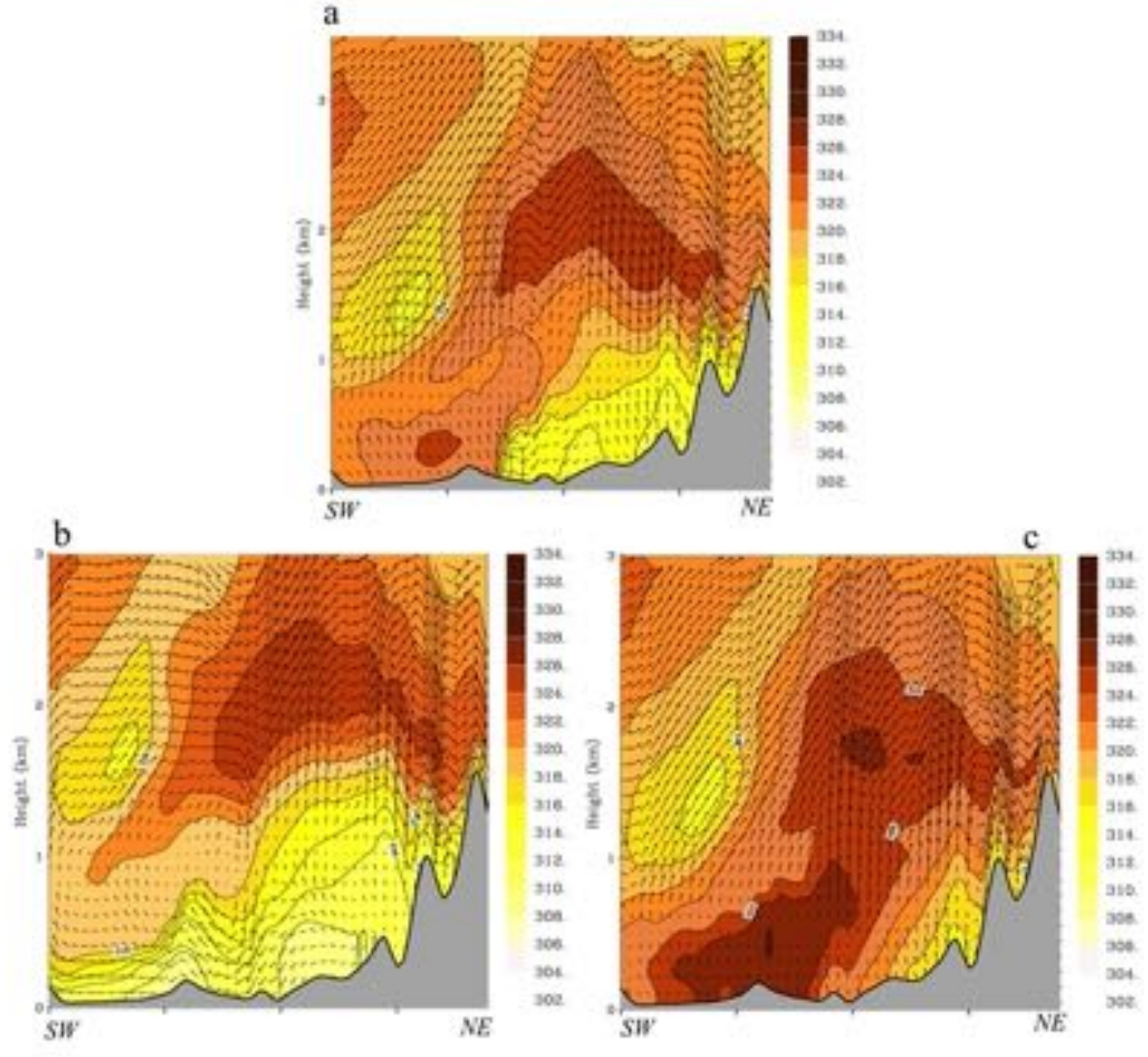
a
b
c
Height (km)
SW
NE
334.
332.
330.
328.
326.
324.
322.
320.
318.
316.
314.
312.
310.
308.
306.
304.
302.

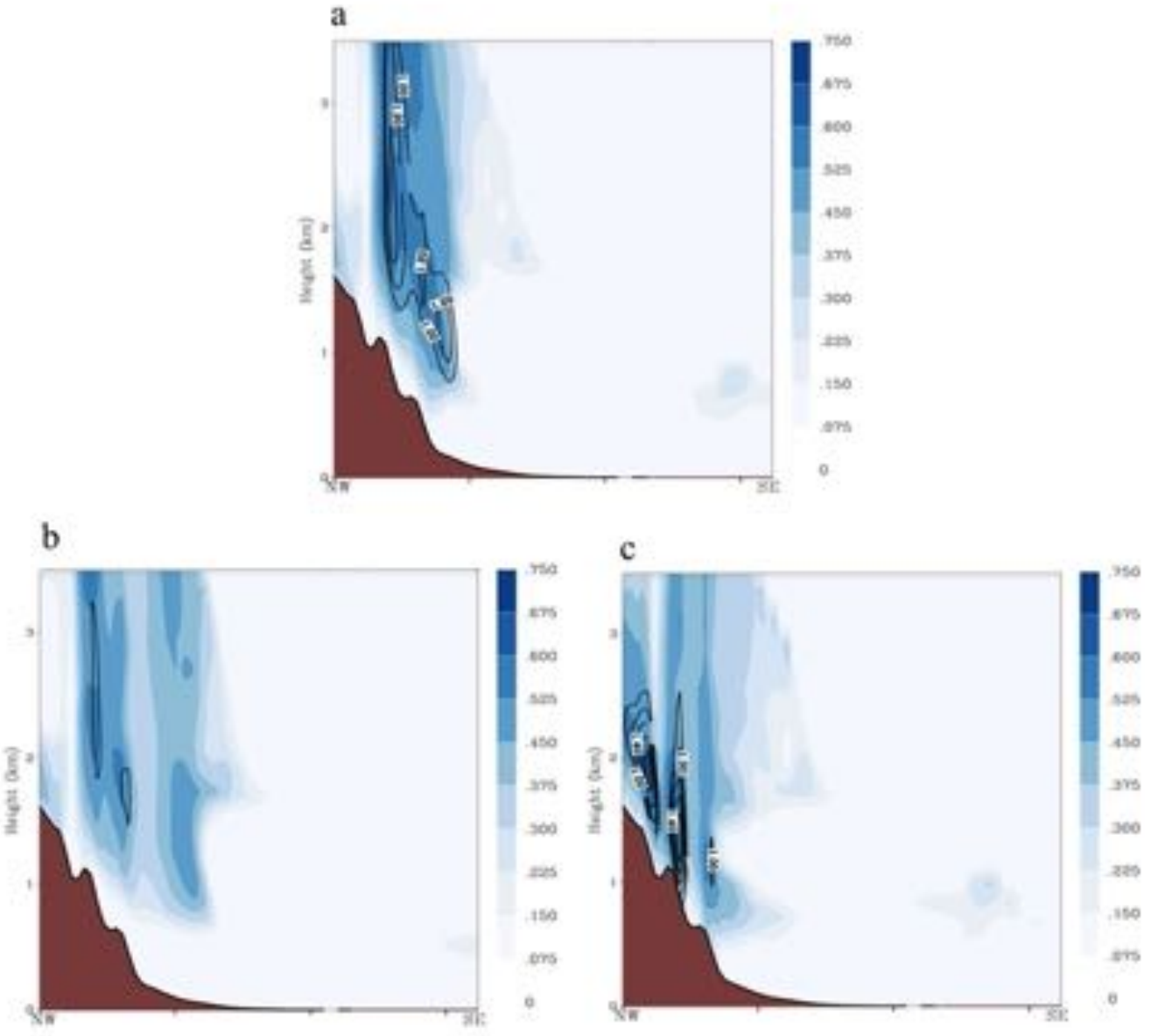
a
b
c
Height (km)
NW
SE
.750
.675
.600
.525
.450
.375
.300
.225
.150
.075
0

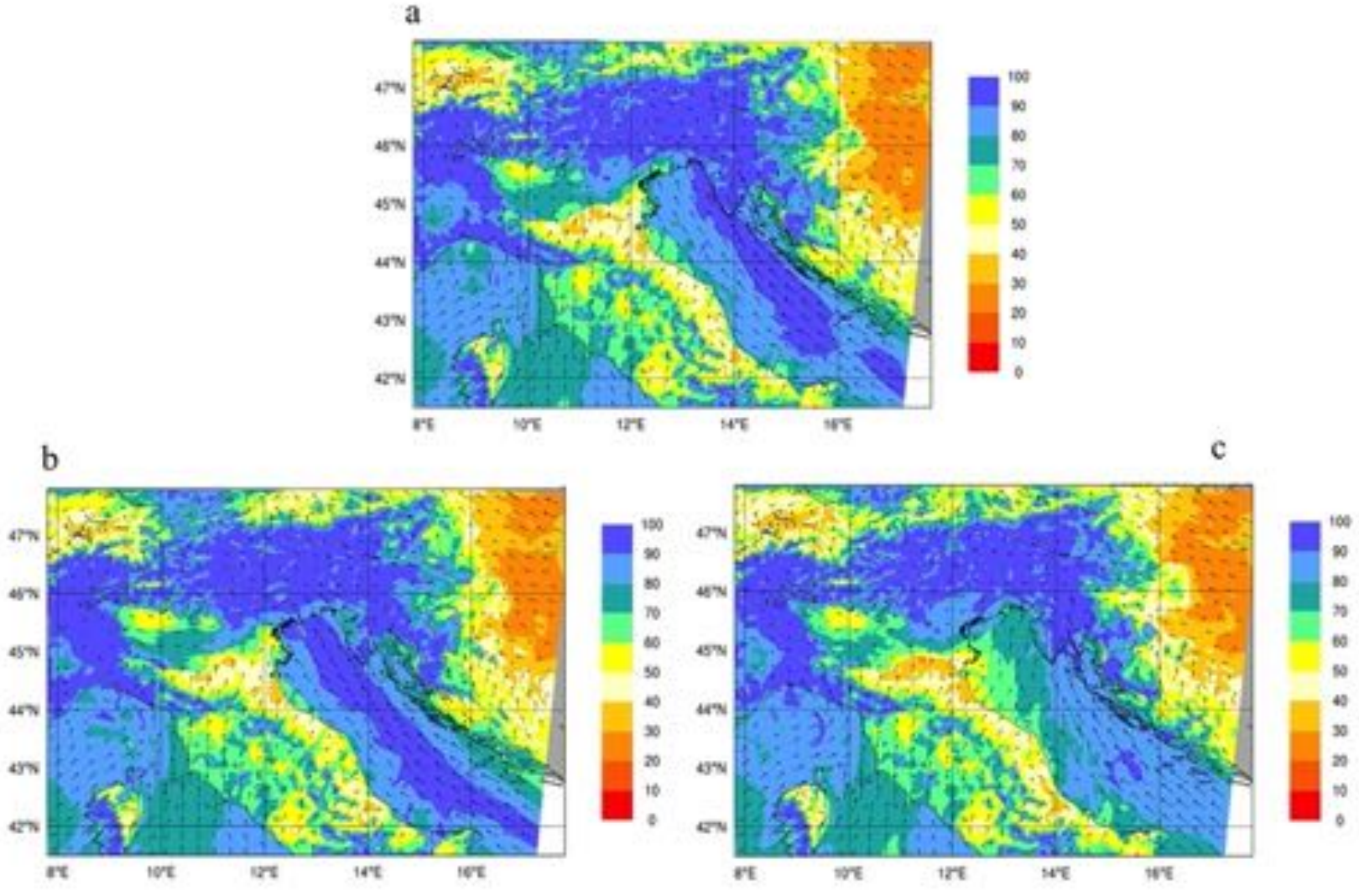
a
b
c
47°N
46°N
45°N
44°N
43°N
42°N
8°E
10°E
12°E
14°E
16°E
100
90
80
70
60
50
40
30
20
10
0

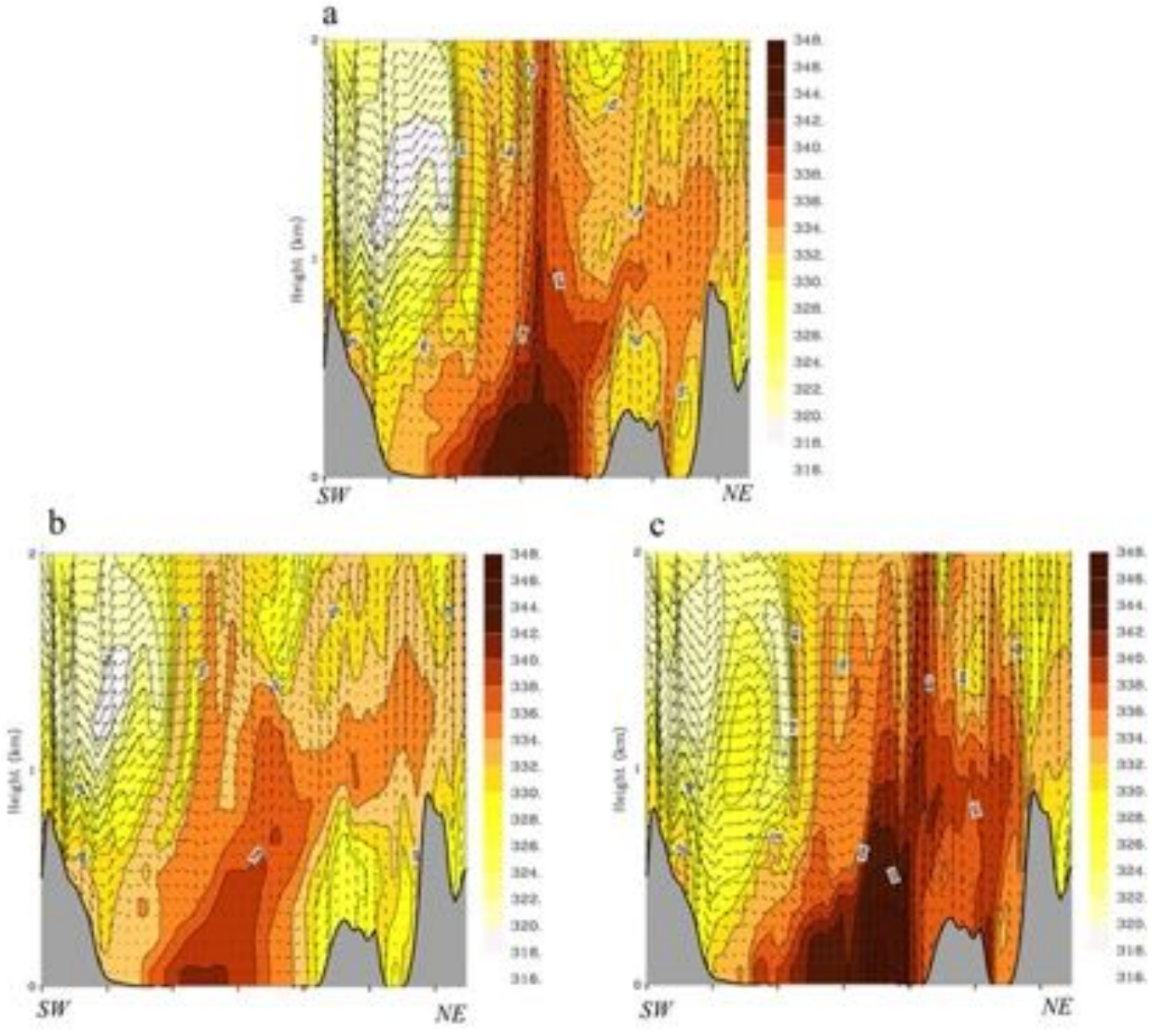
a
b
c
SW
NE
Height (km)

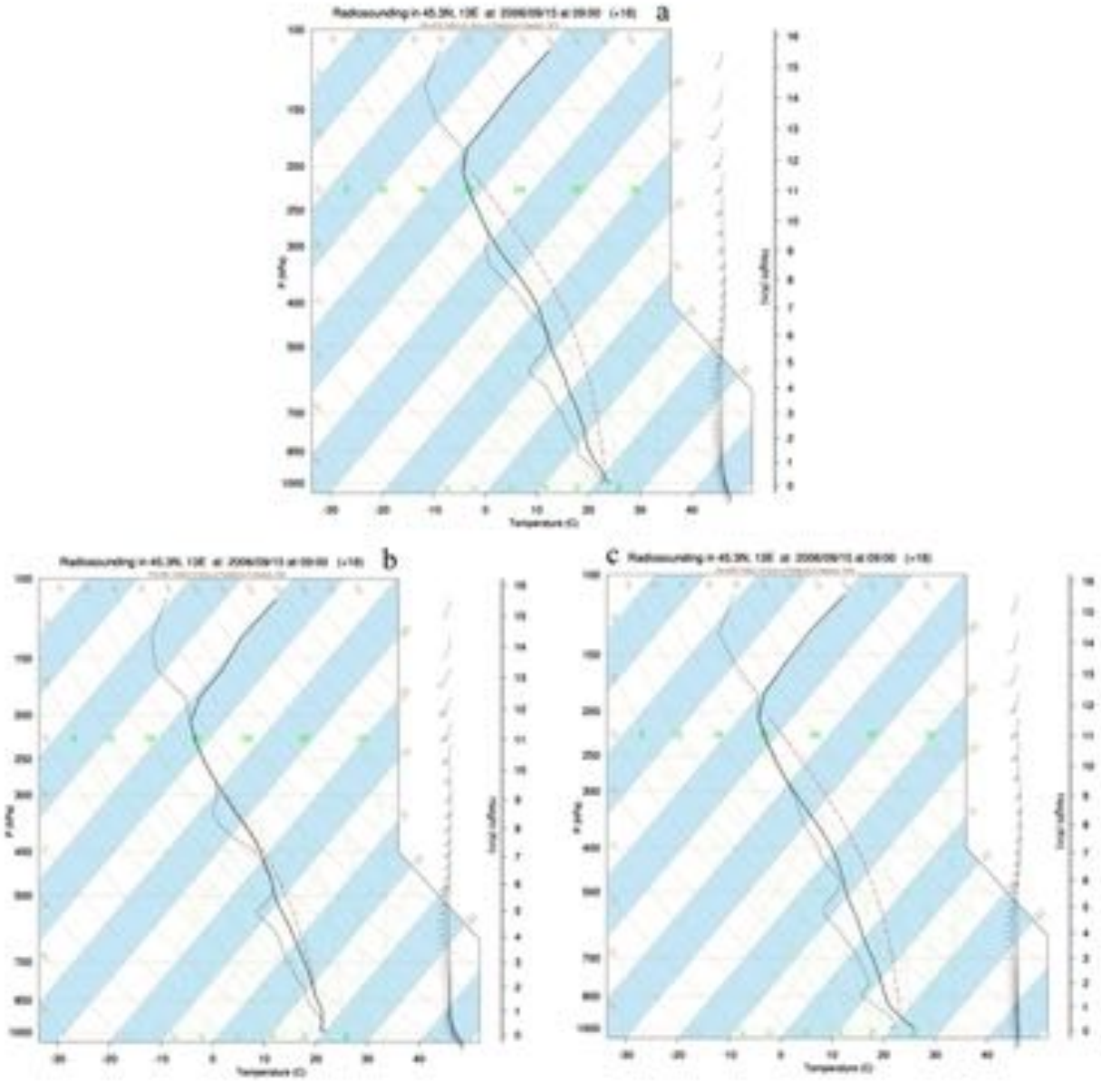
a
b
c

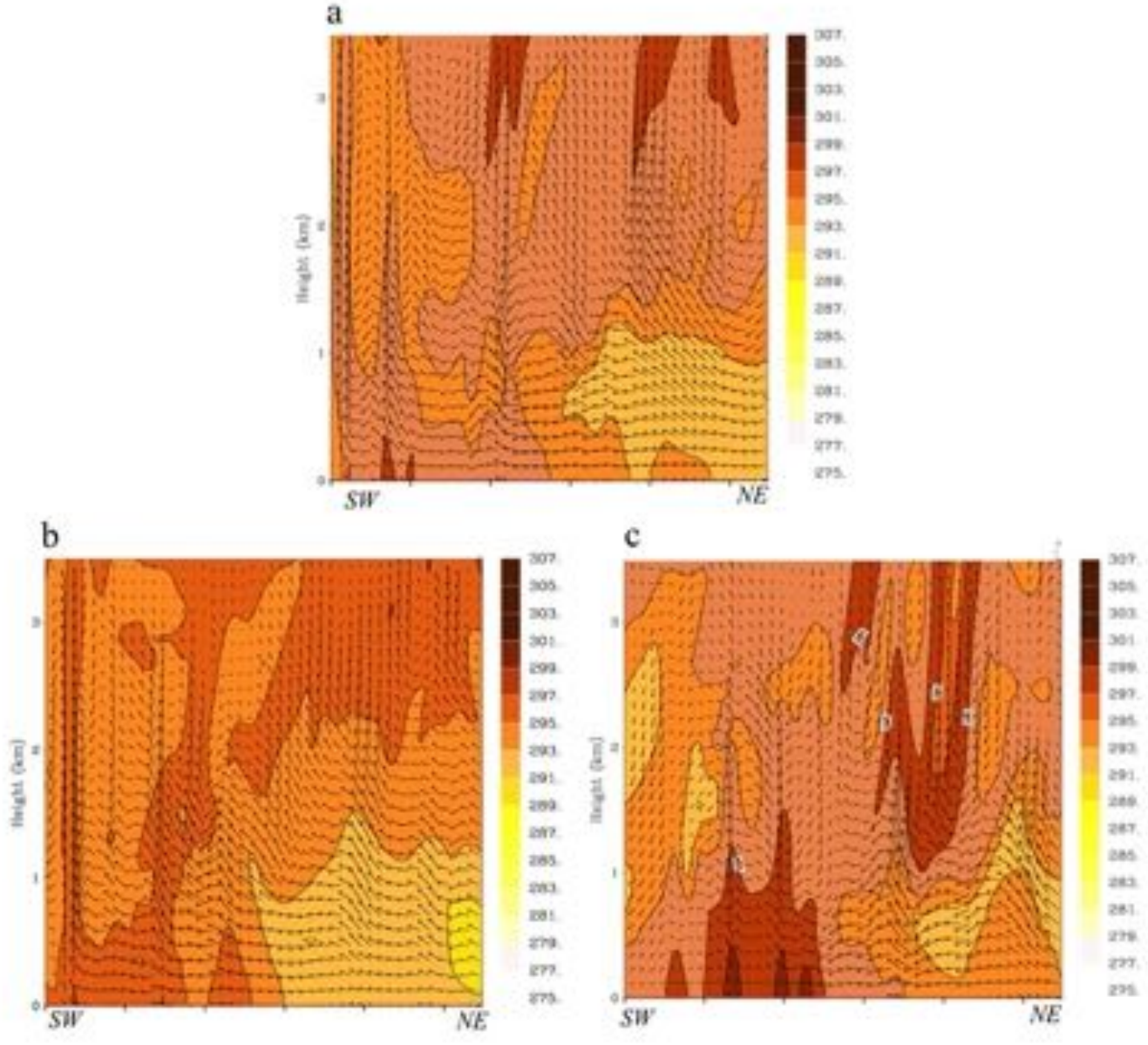
a
b
c
Height (km)
SW
NE
307.
305.
303.
301.
299.
297.
295.
293.
291.
289.
287.
285.
283.
281.
279.
277.
275.

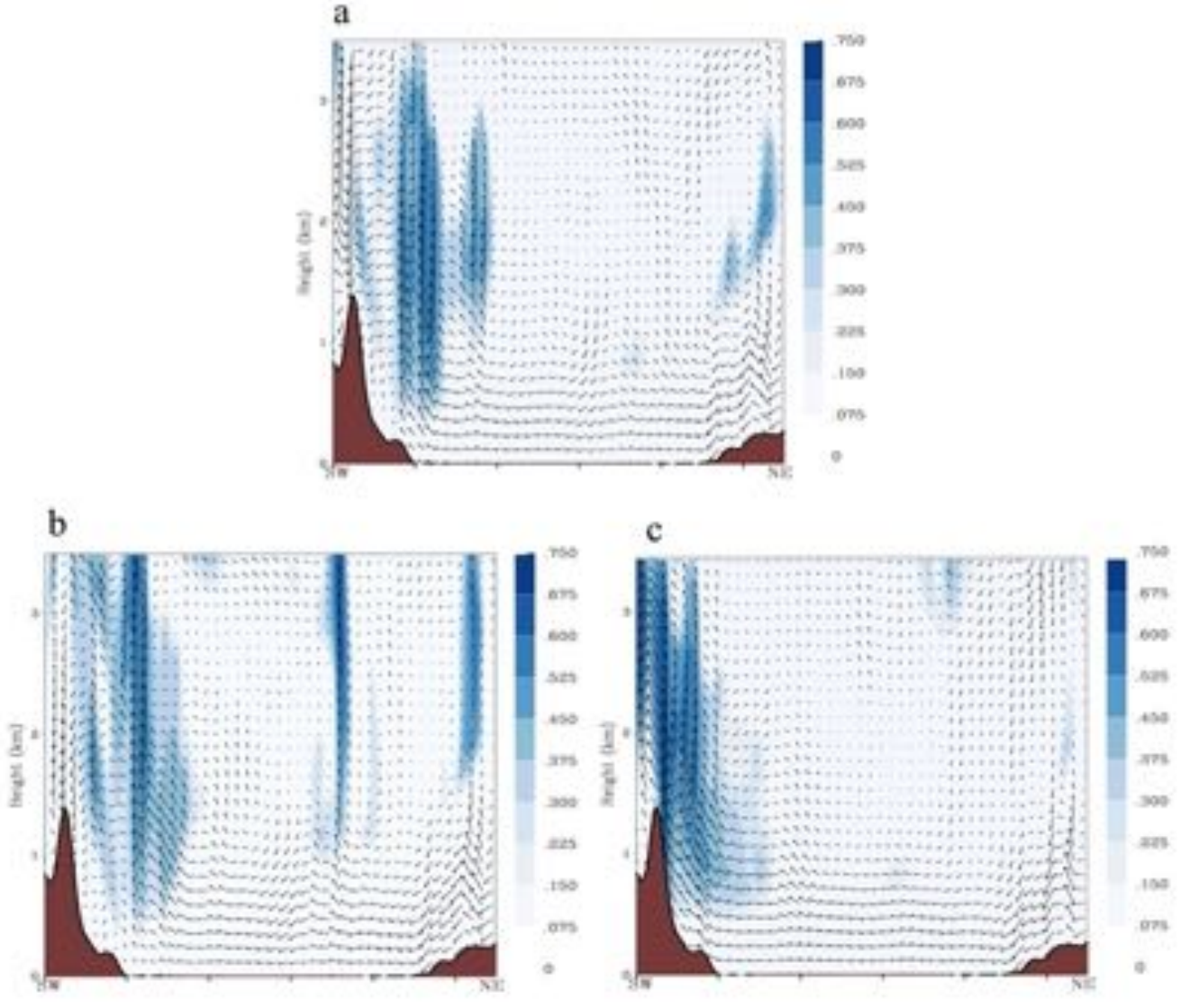
a
b
c
Height (km)
SW
NE
750
675
600
525
450
375
300
225
150
075
0

Case study	Bolam initial condition	Accumulated rainfall period	Type of event	Max LH flux contribution (W)
SIR-01	10 Nov. 2012 1200 UTC	11 Nov. 0000 UTC – 12 Nov. 0000 UTC	Sirocco and orographic precipitation	2.19×10^{12}
SIR-02	30 Oct. 2010 1800 UTC	31 Oct. 1200 UTC – 01 Nov. 1200 UTC	Sirocco and orographic precipitation	1.51×10^{12}
SIR-03	14 Sep. 2006 1200 UTC	15 Sep. 0000 UTC – 16 Sep. 0000 UTC	Sirocco and convective precipitation	2.44×10^{12}
BOR-01	9 Feb. 2012 1200 UTC	10 Feb. 0000 UTC – 11 Feb. 0000 UTC	Cyclonic Bora	1.38×10^{13}
BOR-02	13 Sep. 2012 1200 UTC	14 Sep. 0000 UTC – 15 Sep. 0000 UTC	Cyclonic Bora	1.94×10^{13}
BOR-03	30 Dec. 2014 0000 UTC	31 Dec. 0000 UTC – 01 Jan. 0000 UTC	Anticyclonic Bora	1.94×10^{13}

Table 1: Selected Sirocco and Bora events. Initial conditions for BOLAM simulations (MOLOCH is initialized 3 hours later) are reported, together with the indication of the period of intense precipitation and of the type of event. The last column shows the maximum contribution to the atmospheric water budget provided by the surface latent heat fluxes from Adriatic Sea (see Sect. 5.2.2).

Highlights

- Numerical simulations of heavy precipitation associated with intense air-sea interaction over the Adriatic Sea.
- Sensitivity of forecast precipitation to SST uncertainty.
- The response of intense precipitation patterns to SST uncertainties is complex.
- SST impact on dynamics and on orographic flow regime and, in turn, on precipitation.